

Counterfactual Supervision-based Information Bottleneck for Out-of-Distribution Generalization

Bin Deng and Kui Jia

South China University of Technology
eebindeng@mail.scut.edu.cn

16 Aug 2022

Abstract

Learning invariant (causal) features for out-of-distribution (OOD) generalization has attracted extensive attention recently, and among the proposals invariant risk minimization (IRM) [3] is a notable solution. In spite of its theoretical promise for linear regression, the challenges of using IRM in linear classification problems yet remain [41, 31]. Along this line, a recent study [1] has made a first step and proposes a learning principle of information bottleneck based invariant risk minimization (IB-IRM). In this paper, we first show that the key assumption of support overlap of invariant features used in [1] is rather strong for the guarantee of OOD generalization and it is still possible to achieve the optimal solution without this assumption. To further answer the question of whether IB-IRM is sufficient for learning invariant features in linear classification problems, we show that IB-IRM would still fail in two cases whether or not the invariant features capture all information about the label. To address such failures, we propose a *Counterfactual Supervision-based Information Bottleneck (CSIB)* learning algorithm that provably recovers the invariant features. The proposed algorithm works even when accessing data from a single environment, and has theoretically consistent results for both binary and multi-class problems. We present empirical experiments on three synthetic datasets that verify the efficacy of our proposed method.

1 Introduction

Current machine learning models often fail to generalize when domain distributions of testing data differ from the training ones. This phenomenon has been repeatedly witnessed and intentionally exposed in many examples [45, 40, 15, 33, 17]. Among the explanations, shortcut learning [14] is considered as a main factor causing this phenomenon. A nice example is about the classification of images of cows and camels — a trained convolutional network tends to recognize cows or camels by learning spurious features from image backgrounds (e.g., green pastures for cows and deserts for camels), rather than learning the causal shape features of the animals [5]; decisions based on the spurious features would make the learned models fail when cows or camels appear in unusual, different environments. Machine learning models are expected to have the capability of out-of-distribution (OOD) generalization and avoid shortcut learning.

To achieve OOD generalization, recent theories [3, 22, 2, 37, 1] are motivated by causality literature [34, 36], and resort to extraction of the invariant, causal features and establishing the relevant conditions under which machine learning models have the guaranteed generalization. Among these works, invariant risk minimization (IRM) [3] is a notable learning paradigm that incorporates the invariance principle [35] into practice. In spite of the theoretical promise of IRM, it is only applicable to problems of linear regression. For other problems such as linear classification, Ahuja et al. [1] first show that for OOD generalization, linear classification is more difficult in the case when invariant features capture all information about the label, and propose a new learning method of information bottleneck-based invariant risk minimization (IB-IRM). In this work, we closely investigate the conditions identified in [1] and propose improved results for OOD generalization of linear classification. Our technical contributions are as follows.

Contributions. In [1], a notion of support overlap of invariant features is assumed in order to make the OOD generalization of linear classification successful. In this work, we first show that this

assumption is rather strong and it is still possible to achieve such goal without this assumption. Then, we examine whether the IB-IRM proposed in [1] is sufficient to learn invariant features for linear classification, and find that IB-IRM still fails in several cases whether or not the invariant features capture all information of the label. We then analyze two failure modes of IB-IRM, in particular when the spurious features in training environments capture sufficient information for the label but less than the invariant features. Based on the above analyses, we propose a new method, termed counterfactual supervision-based information bottleneck (CSIB), to address such failures. We prove that, under the proposed weaker assumptions, CSIB is theoretically guaranteed for the success of OOD generalization in linear classification. Notably, CSIB works even when accessing data from a single environment, and has theoretically consistent results for both binary and multi-class problems. Finally, we design three synthetic datasets based on our used motivating examples; experiments verify our proposed method empirically. All the proofs and details of experiments are given in the appendices.

2 OOD generalization for linear classification: background and failures

We consider the same learning setting as in [3, 1], but focus on the linear classification problem only. Let $D = \{D^e\}_{e \in \mathcal{E}_{tr}}$ be the training data gathered from a set of training environments \mathcal{E}_{tr} , where $D^e = \{(x_i^e, y_i^e)\}_{i=1}^{n_e}$ is the dataset from environment e with each instance (x_i^e, y_i^e) i.i.d. drawn from $\mathbb{P}(X^e, Y^e)$. Let $\mathcal{X}^e \subseteq \mathbb{R}^d$ and $\mathcal{Y} \subseteq \{0, 1\}$ (or $\mathcal{Y} \subseteq \{-1, 1\}$) be the support sets of the input feature values and output labels in the environment e , respectively. Given observed data D , the goal of OOD generalization is to find a predictor $f: \mathbb{R}^d \rightarrow \mathcal{Y}$ from \mathcal{F} such that it can perform well across a large set of unseen but related environments $\mathcal{E}_{all} \supset \mathcal{E}_{tr}$. Formally, it is expected to minimize

$$\min_{f \in \mathcal{F}} \max_{e \in \mathcal{E}_{all}} R^e(f), \quad (1)$$

where $R^e(f) := \mathbb{E}_{X^e, Y^e}[l((X^e, Y^e), f)]$ is the risk under the environment e with $l(\cdot, \cdot)$ the well defined loss function. Clearly, without any restrictions on \mathcal{E}_{all} , it is impossible to achieve OOD generalization. We first follow the structure equation model (SEM) used in [1] and review some results it has made.

Assumption 1 (Linear classification SEM (FIIF)). *In each $e \in \mathcal{E}_{all}$*

$$\begin{aligned} Y^e &\leftarrow \mathbf{1}(w_{inv}^* \cdot Z_{inv}^e) \oplus N^e, \quad N^e \sim \text{Bernoulli}(q), \quad q < \frac{1}{2}, \quad N^e \perp (Z_{inv}^e, Z_{spu}^e), \\ X^e &\leftarrow S(Z_{inv}^e, Z_{spu}^e), \end{aligned} \quad (2)$$

where $w_{inv}^* \in \mathbb{R}^m$ with $\|w_{inv}^*\| = 1$ is the labeling hyperplane, $Z_{inv}^e \in \mathbb{R}^m$, $Z_{spu}^e \in \mathbb{R}^o$, N^e is binary noise with identical distribution across environments, \oplus is the XOR operator, S is invertible, and $\mathbf{1}(x) = 1$ if $x > 0$ otherwise 0.

Following [1], we say the invariant features Z_{inv}^e in a directed acyclic graph (DAG) are called the fully informative invariant features (FIIF) if we have $Y^e \perp X^e | Z_{inv}^e$. Otherwise we call it partially informative invariant features (PIIF). The above assumption shows how the environment data (X^e, Y^e) are generated from the latent invariant features Z_{inv}^e and spurious features Z_{spu}^e , and obviously, the invariant features Z_{inv}^e in Assumption 1 are fully informative to Y^e . The DAG corresponding to this assumption is illustrated in Fig. 1(a).

To solve Eq. (1), the objectives of IRM [3] and IB-IRM [1] are listed as follows (we consider a homogenous linear classifier w here for convenience):

$$\text{IRM: } \min_{w, \Phi} \frac{1}{|\mathcal{E}_{tr}|} \sum_{e \in \mathcal{E}_{tr}} R^e(w \cdot \Phi), \quad \text{s.t. } w \in \arg \min_{\tilde{w}} R^e(\tilde{w} \cdot \Phi), \forall e \in \mathcal{E}_{tr}. \quad (3)$$

$$\text{IB-IRM: } \min_{w, \Phi} \sum_{e \in \mathcal{E}_{tr}} h^e(w \cdot \Phi) \quad \text{s.t. } \frac{1}{|\mathcal{E}_{tr}|} \sum_{e \in \mathcal{E}_{tr}} R^e(w \cdot \Phi) \leq r^{th}, w \in \arg \min_{\tilde{w}} R^e(\tilde{w} \cdot \Phi), \forall e \in \mathcal{E}_{tr}, \quad (4)$$

where $h^e(f) = H(f(X^e))$ with the H the Shannon entropy (or a lower bounded differential entropy) and r^{th} is the threshold on the average risk. If we drop the invariance constraint from IRM and IB-IRM,

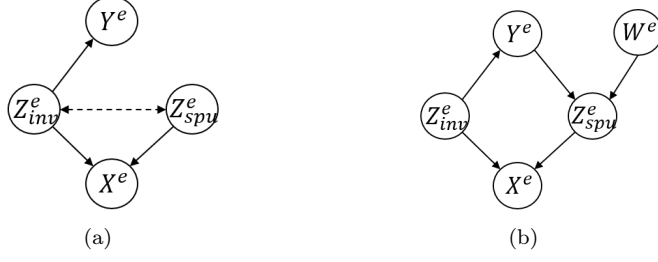


Figure 1: (a) DAG of Assumption 1. (b) DAG of Assumption 7. In (a), the invariant features are called the fully informative invariant features (FIIF) because $Y^e \perp X^e | Z_{inv}^e$, while in (b) they are called partial informative invariant features (PIIF).

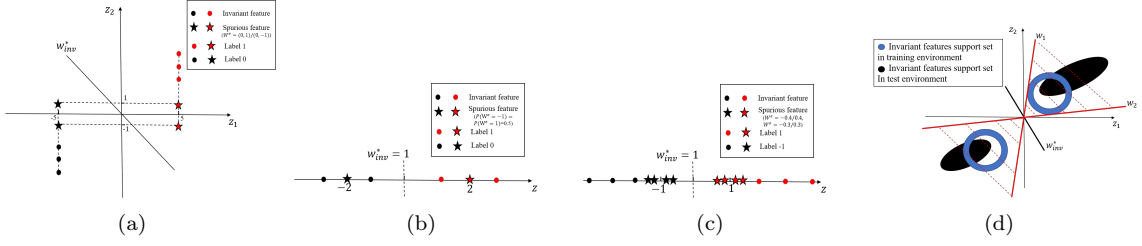


Figure 2: (a) Example 1. (b) Example 2. (c) Example 3. (d) Here, we assume we have only two environments in total. The blue and black regions represent the support set in training and test environments respectively. Although their support sets do not overlap, a zero-error classifier on the training environment data would clearly make the test error zero, thus enables the OOD generalization.

we get standard empirical risk minimization (ERM) and information bottleneck-based empirical risk minimization (IB-ERM) respectively. The use of entropy constraint in IB-IRM is inspired from the information bottleneck principle [47] where mutual information $I(X; \Phi(X))$ is used for information compression. Since the representation $\Phi(X)$ is a deterministic mapping of X , minimizing the entropy of $\Phi(X)$ is equivalent to minimizing the mutual information $I(X; \Phi(X))$. In brief, the optimization of IB-IRM is to pick the one that has the least entropy among all highly predictive invariant predictors. Let us define the support set of the invariant (*resp.*, spurious) features Z_{inv}^e (*resp.*, Z_{spu}^e) in environment e as \mathcal{Z}_{inv}^e (*resp.*, \mathcal{Z}_{spu}^e).

Assumption 2 (Bounded invariant features). $\cup_{e \in \mathcal{E}_{tr}} \mathcal{Z}_{inv}^e$ is a bounded set¹.

Assumption 3 (Bounded spurious features). $\cup_{e \in \mathcal{E}_{tr}} \mathcal{Z}_{spu}^e$ is a bounded set.

Assumption 4 (Invariant feature support overlap). $\forall e \in \mathcal{E}_{all}, \mathcal{Z}_{inv}^e \subseteq \cup_{e' \in \mathcal{E}_{tr}} \mathcal{Z}_{inv}^{e'}$.

Assumption 5 (Strictly separable invariant features). $\rho_{inv} = \min_{z \in \cup_{e \in \mathcal{E}_{tr}} \mathcal{Z}_{inv}^e} \text{sgn}(w_{inv}^* \cdot z)(w_{inv}^* \cdot z) > 0$.

Under the above assumptions, we now present the main OOD generalization results from [1] for linear classification.

Theorem 1 (Impossibility of guaranteed OOD generalization for linear classification [1]). *Suppose each $e \in \mathcal{E}_{all}$ follows Assumption 1. If for all the training environments \mathcal{E}_{tr} , the latent invariant features are bounded and strictly separable, i.e., Assumption 2 and 5 hold, then every deterministic algorithm fails to solve the OOD generalization (Eq. 1).*

Based on the above theorem, it is claimed in [1] that without the support overlap assumption (Assumption 4) on the invariant features, OOD generalization is impossible for linear classification and therefore requires the Assumption 4 for all of the rest analyses. However, we would show that such an assumption is rather strong. For example, consider a generalization task in a single environment without spurious features, requiring the assumption of support overlap between training data and test data

¹A set \mathcal{Z} is bounded if $\exists M < \infty$ such that $\forall z \in \mathcal{Z}, \|z\| \leq M$.

would promote the algorithm for memorization instead of generalization, which is a little trivial to our topic. With such concerns, we propose a much weaker assumption that is highly related to the learning hypothesis space and connects the traditional generalization theory [42]. To help the illustration, we first give an intuitive example as shown in Figure 2(d), where the learning hypothesis space is the set of linear hyperplanes; clearly, although the support sets of invariant features between training and test environments are different, it would be still possible for the success of OOD generalization if the invariant features are learned.

Let $\mathbb{P}^{tr}(X_{inv}, Y) = \frac{1}{|\mathcal{E}_{tr}|} \sum_{e \in \mathcal{E}_{tr}} \mathbb{P}(X_{inv}^e, Y^e)$ be the mixture distribution of invariant features in the training environments, $\mathcal{A} = \{w \in \mathbb{R}^m | \|w\| = 1\}$, and $l((X, Y), a) = \mathbb{I}[a(X) \neq Y]$ (denote as 0-1 loss for convenience). We now present a weaker assumption to the invariant features.

Assumption 6. $\forall e \in \mathcal{E}_{all}, A_l(\mathbb{P}^{tr}(X_{inv}), Y) \subseteq A_l(\mathbb{P}(X_{inv}^e, Y^e))$, where $A_l(p) = \arg \min_{a \in \mathcal{A}} \mathbb{E}_p[l(X, a)]$ with $l : \mathcal{X} \times \mathcal{A} \rightarrow \mathbb{R}$ the 0-1 loss function.

Clearly, under the assumption of separable invariant features (Assumption 5), if Assumption 4 holds, Assumption 6 would also hold, but not vice versa. We would show that Assumption 6 can be substituted for Assumption 4 for the guarantee of OOD generalization in our proposed method later. Before that, we review another main result presented in [1].

Theorem 2 (IB-IRM and IB-ERM vs. IRM and ERM [1]). *Suppose each $e \in \mathcal{E}_{all}$ follows Assumption 1. Assume that the invariant features are strictly separable, bounded, and satisfy support overlap, i.e., Assumptions 2, 4, and 5 hold. Also, for each $e \in \mathcal{E}_{tr}, Z_{spu}^e \leftarrow AZ_{inv}^e + W^e$, where $A \in \mathbb{R}^{o \times m}$, $W^e \in \mathbb{R}^o$ is continuous (or discrete with each component at least two distinct values), bounded, and zero mean noise. Each solution to IB-IRM (Eq. (4)) with l as 0-1 loss and $r^{th} = q$, and IB-ERM solves the OOD generalization (Eq. (1)) but ERM and IRM (Eq. (3)) fail.*

We would show that IB-IRM could fail in many cases; we here present an illustrating example of such a failure.

Example 1. *Following Assumption 1, and let $Z_{spu}^e \leftarrow AZ_{inv}^e + W^e$ with $A = [1, 0; 0, 0]$ and $W^e \in \mathbb{R}^2$ varies in different environments. For any environment $e \in \mathcal{E}_{all}$, we assume that the distribution of Z_{inv}^e and N^e does not change. As shown in Fig. 2(a), $w_{inv}^* = (\frac{\sqrt{2}}{2}, \frac{\sqrt{2}}{2})$ and Z_{inv}^e is a discrete distribution uniformly on six points $((-5, -4), (-5, -5), (-5, -6), (5, 4), (5, 5), (5, 6))$. Now we can construct the training data of two environments:*

$$\mathcal{E}_{tr} = \{\text{replace } W^e \text{ by } (0, 1), \text{ replace } W^e \text{ by } (0, -1)\}$$

Then, by applying IB-IRM to the above example with l as 0-1 loss and $r^{th} = q$, we would get a model of $f = \mathbf{1} \circ \Phi^*$ as $\Phi^* = (w \cdot \Phi)$. Consider the prediction made by this model as (we ignore classifier bias here for convenience)

$$\Phi^* \cdot X^e = \Phi^* \cdot S(Z_{inv}^e, Z_{spu}^e) = \Phi_{inv} \cdot Z_{inv}^e + \Phi_{spu} \cdot Z_{spu}^e. \quad (5)$$

It is trivial to show that the Φ^* of $\Phi_{inv} = \mathbf{0}$ and $\Phi_{spu} = (\frac{\sqrt{2}}{2}, \frac{\sqrt{2}}{2})$ is an invariant predictor across training environments with classification error $\frac{1}{|\mathcal{E}_{tr}|} \sum_{e \in \mathcal{E}_{tr}} R^e = q$, and it achieves the least entropy of $h^e = \log 2$ for each training environment e , and therefore, it is a solution of IB-IRM. However, since the predictor of Φ^* relies on spurious features that may change arbitrarily on unseen environments, it thus fails to solve the OOD generalization problem (Eq. (1)).

Understanding the failures: Although the Example 1 satisfies Assumptions 2, 3, 4, and 5, we find that it is still insufficient for IB-IRM to success, appearing as a contradiction to Theorem 2. It is worth to note that this contradiction is due to the different condition of W^e . This is because, in Example 1, W^e is a delta distribution or discrete distribution supported on only one point, while in Theorem 2, it requires the W^e to be a variable that has at least two distinct values with zero mean noise in each component, which usually does not hold in practice especially when the dimension of spurious features is high. For example, if we replace the W^e in Example 1 with two distinct values of (α, β) and $(-\alpha, -\beta)$, with probability 0.5 each, and set two environments of $(\alpha = 0, \beta = 1)$ and $(\alpha = 0, \beta = 2)$, we can still conclude that IB-IRM may fail by setting $\Phi_{inv} = \mathbf{0}$ and $\Phi_{spu} = (1, 0)$. Then, what is the true reason behind this? We state that the reason is that the invariant features are not the minimal sufficient statistics for the label. In this case, IB-IRM may fail when the spurious features in the training environments capture less information but sufficient for the label. We would formally state that as follow.

Theorem 3. *Following Assumption 1, assume that a) the invariant features are strictly separable, bounded, and satisfy support overlap (Assumptions 2, 4, and 5 hold), b) the invariant features are discrete variables with at least three distinct points (not on the same line) and support overlap in each training environment. Then, there exists at least one pair of $(w \in \mathbb{R}^m, b \in \mathbb{R})$ such that the transformed variables $T_{inv}^e = w \cdot Z_{inv}^e + b$ are still bounded and satisfy support overlap, and satisfy $\text{sgn}(T_{inv}^e) = \text{sgn}(w_{inv}^* \cdot Z_{inv}^e)$ and $H(T_{inv}^e) < H(Z_{inv}^e)$ for any $e \in \mathcal{E}_{tr}$.*

When there exists a component of W^e (assume the k -th component $W^e[k]$) such that for all training environments, $W^e[k]$ is a delta distribution or discrete distribution supported on only one point, then we have $\sum_{e \in \mathcal{E}_{tr}} H(T_{inv}^e) = \sum_{e \in \mathcal{E}_{tr}} H(T_{inv}^e + w_{spu} \cdot W^e[k]) < \sum_{e \in \mathcal{E}_{tr}} H(Z_{inv}^e)$ for any $w_{spu} \in \mathbb{R}$. From the above theorem, we can see that when the spurious features in the training environments include the T_{inv}^e information and $W^e[k]$ supports on only one point for some k , IB-IRM or IB-ERM methods would prefer to select these spurious features (also with a non-zero weight to $W^e[k]$) due to the smaller entropy, and thus may fail to generalize to unseen environments where spurious features change (due to the change of $W^e[k]$). Note that we only analyse the discrete distribution of Z_{inv}^e here for convenience. The conclusions for the continuous distribution are similar.

In the above example, we have shown a failure case of IB-IRM when the condition assumed on W^e is lightly violated. We now move to another failure mode of IB-IRM even when this assumption is satisfied, i.e., W^e is zero-mean with each component at least two distinct points, on both the FIIF and PIIF cases. We first show the FIIF case below.

Example 2. *Following Assumption 1, and let $Z_{inv}^e \leftarrow AZ_{spu}^e + W^e$ with $m = o = 1$ and $A = 1$, and $W^e \in \mathbb{R}$ is zero-mean with at least two distinct points, where Z_{spu}^e and W^e may vary in different environments. For any environment $e \in \mathcal{E}_{all}$, we assume that the distribution of N^e does not change. As shown in Fig. 2(b), $w_{inv}^* = 1$ is the generated classifier. Now we can construct the training data of two environments:*

$$\mathcal{E}_{tr} = \{Z_{spu}^e = -2, Z_{spu}^e = 2\}$$

and set $W^e = -1$ or 1 with probability 0.5 each in \mathcal{E}_{tr} .

Then, by applying IB-IRM to the above example with l as 0-1 loss and $r^{th} = q$, we would get a model of $f = \mathbf{1} \circ \Phi^*$ as $\Phi^* = (w \cdot \Phi)$. Consider the prediction made by this model as (we ignore the bias here for convenience)

$$\Phi^* \cdot X^e = \Phi^* \cdot S(Z_{inv}^e, Z_{spu}^e) = \Phi_{inv} \cdot Z_{inv}^e + \Phi_{spu} \cdot Z_{spu}^e. \quad (6)$$

It is trivial to show that the Φ^* of $\Phi_{inv} = 0$ and $\Phi_{spu} = 1$ is an invariant predictor across training environments with classification error $\frac{1}{|\mathcal{E}_{tr}|} \sum_{e \in \mathcal{E}_{tr}} R^e = 0$, and it achieves the least entropy of $h^e = 0$ for each training environment e , and therefore, it is a solution of IB-IRM. However, since the predictor of Φ^* relies on spurious features which may change arbitrarily on unseen environments, it thus fails to solve the OOD generalization problem (Eq. (1)).

We now move to the PIIF case as follows.

Assumption 7 (Linear classification SEM (PIIF)). *In each $e \in \mathcal{E}_{all}$*

$$\begin{aligned} Y^e &\leftarrow 2(\mathbf{1}(w_{inv}^* \cdot Z_{inv}^e) \oplus N^e) - 1, \quad N^e \sim \text{Bernoulli}(q), \quad q < \frac{1}{2}, \quad N^e \perp Z_{inv}^e, \\ Z_{spu}^e &= AY^e + W^e, \quad X^e \leftarrow S(Z_{inv}^e, Z_{spu}^e), \end{aligned} \quad (7)$$

where $w_{inv}^* \in \mathbb{R}^m$ with $\|w_{inv}^*\| = 1$ is the labeling hyperplane, $Z_{inv}^e \in \mathbb{R}^m$, $Z_{spu}^e \in \mathbb{R}^o$, $A \in \mathbb{R}^{o \times 1}$, N^e is binary noise with identical distribution across environments, $W^e \in \mathbb{R}^o$ is continuous (or discrete variable with each component at least two distinct values), bounded, and zero mean, which varies in different environments, \oplus is the XOR operator, and S is invertible.

The DAG of the above assumption can be seen in Fig. 1(b).

Example 3. *Following Assumption 7, let $m = o = 1$, $w_{inv}^* = 1$, $A = 1$, and Z_{inv}^e is a discrete distribution uniformly on six points $(-4, -3, -2, 2, 3, 4)$. For any environment $e \in \mathcal{E}_{all}$, we assume that the distribution of Z_{inv}^e and N^e does not change, as shown in Fig. 2(c). Now we can construct the training data of two environments:*

$$\mathcal{E}_{tr} = \{P(W^e = 0.4) = P(W^e = -0.4) = 0.5, P(W^e = 0.3) = P(W^e = -0.3) = 0.5\}$$

Then, by applying IB-IRM to the above example with l as 0-1 loss and $r^{th} = q$, we would get a model of $f = \mathbf{sgn} \circ \Phi^*$ as $\Phi^* = (w \cdot \Phi)$. Consider the prediction made by this model as (we ignore classifier bias here for convenience)

$$\Phi^* \cdot X^e = \Phi^* \cdot S(Z_{inv}^e, Z_{spu}^e) = \Phi_{inv} \cdot Z_{inv}^e + \Phi_{spu} \cdot Z_{spu}^e. \quad (8)$$

Next, we would show that $\Phi_{inv} = 0$ and $\Phi_{spu} \neq 0$, and therefore IB-IRM fails to address the OOD generalization problem (Eq. (1)). Clearly, the results to the above example can be divided into four categories: case 1): $\Phi_{inv} = 0$ and $\Phi_{spu} \neq 0$; case 2): $\Phi_{inv} \neq 0$ and $\Phi_{spu} \neq 0$; case 3): $\Phi_{inv} \neq 0$ and $\Phi_{spu} = 0$; case 4): $\Phi_{inv} = 0$ and $\Phi_{spu} = 0$.

First, it is trivial to show that the case 4) is impossible since the classification error of such predictor is $0.5 > q$, and for each of the rest of three cases, the classification error would be equal to or smaller than q . For example, for the case 1): $\Phi_{inv} = 0$ and $\Phi_{spu} = 1$, the error is 0; for the case 2): $\Phi_{inv} = 1$ and $\Phi_{spu} = 1$, the error is q ; for the case 3): $\Phi_{inv} = 1$ and $\Phi_{spu} = 0$, the error is q .

Second, we would show that the resulting predictor of case 1) of $\Phi_{inv} = 0$ and $\Phi_{spu} = 1$ is an invariant predictor across training environments. This is because, the predictor of $\Phi_{inv} = 0$ and $\Phi_{spu} = 1$ would make $\mathbb{E}[Y^e | Z_{spu}^e = a]$ invariant across two training environments for any $a \in \mathbb{R}$, and thus is a invariant predictor (see Appendix for details of the proof).

Finally, it is trivial to show that the predictor of case 1 has the least entropy among them of cases 1-3. Clearly, in case 1): $h^e = \log 4$; in case 2) and 3): $h^e \geq \log 6$ for each environment e .

Understanding the failures: In the above two examples, the failure of invariance constraint for removing the spurious features out is because the spurious features among all training environments generated from different label values are strictly linearly separable. This could make the predictor relying only on spurious features achieve zero training error and thus be an invariant predictor across training environments. Since the label set is finite (with only two values in binary classification) in classification problems, such phenomenon may exist, while it would not happen in regression problems. We state such failure mode formally as below.

Theorem 4. *Following Assumption 1 or 7, if two sets $\cup_{e \in \mathcal{E}_{tr}} Z_{spu}^e (Y^e = 1)$ and $\cup_{e \in \mathcal{E}_{tr}} Z_{spu}^e (Y^e = -1/0)$ are linearly separable and $H(Z_{inv}^e) > H(Z_{spu}^e)$ on each training environment e , then IB-IRM (and IRM, ERM, or IB-ERM) with any $r^{th} \in \mathbb{R}$ fails to address the OOD generalization problem (Eq. (1)).*

The understanding of Theorem 4 is very intuitive since when the spurious features in the training environments with different labels are linearly separable, there is no algorithm that can distinguish spurious features from invariant features. Although the assumption seems strong for this failure, we would show in Appendix that for high-dimensional data, i.e., o is large (common cases in practice such as image data), if the number of environments $|\mathcal{E}_{tr}| < \frac{o}{2}$, we would have high probability that the conditions in Theorem 4 will satisfy and thus OOD generalization will fail by optimizing IB-IRM. This is because, in o -dimensional space, we would have high probability that o randomly drawn distinct points are linearly separable for any two subsets.

3 Counterfactual Supervision-based information bottleneck

In the above analyses, we have shown several failure cases of IB-IRM for OOD generalization in the linear classification problem. The key failure is due to the learned features that only rely on spurious features. To prevent such failure, we present counterfactual supervision-based information bottleneck (CSIB) learning principle for removing the spurious features iteratively.

Overall, the CSIB first uses IB-ERM to extract features, then we apply two counterfactual interventions on the learned features of any single example and get it two counterfactual examples. If these two counterfactual examples have the same class by human supervision, it is possible that the learned features are spurious features. Then we remove such spurious features and apply the IB-ERM again until only invariant features are learned. The details of CSIB algorithm are illustrated below (let Φ' be an identical matrix initially):

Step 1 (IB-ERM): Apply IB-ERM algorithm to all the training environment data \mathcal{E}_{tr} as:

$$\min_{w, \Phi} \sum_{e \in \mathcal{E}_{tr}} h^e(\Phi) \quad \text{s.t.} \quad \frac{1}{|\mathcal{E}_{tr}|} \sum_{e \in \mathcal{E}_{tr}} R^e(w \cdot \Phi) \leq r^{th} \quad (9)$$

with l the 0-1 loss function.

Step 2 (SVD decomposition): Assume $\Phi^* \in \mathbb{R}^{c \times d}$ and w^* are the feature extractor and classifier learned by IB-ERM and the rank of Φ^* is r . We first do singular value decomposition (SVD) to Φ^* and get $\Phi^* = U\Lambda V^T$ with orthogonal matrixes $U \in \mathbb{R}^{c \times c}$ and $V \in \mathbb{R}^{d \times d}$, which can be partitioned by $\Phi^* = [U_1, U_2][\Lambda_1, \mathbf{0}; \mathbf{0}, \mathbf{0}][V_1^T; V_2^T]$ with $U_1 \in \mathbb{R}^{c \times r}$ and $U_2 \in \mathbb{R}^{c \times (d-r)}$, $\Lambda_1 \in \mathbb{R}^{r \times r}$ is the diagonal matrix with r non-zero elements, and $V_1^T \in \mathbb{R}^{r \times d}$ and $V_2^T \in \mathbb{R}^{(d-r) \times d}$.

Step 3 (Counterfactual supervision): Pick a random sample $x \in \mathbb{R}^d$ from training environment with ground truth label y . Assume that input data are bounded by M , then construct two new features z^1 and z^2 by the following operation: $do(z_{1:r}^1) = [-M, \dots, -M]$ and $do(z_{r+1:d}^1) = V_2^T x$; $do(z_{1:r}^2) = [M, \dots, M]$ and $do(z_{r+1:d}^2) = V_2^T x$. Backward the new features z^1 and z^2 to the input space as $x^1 = Vz^1$ and $x^2 = Vz^2$. If the label of x^1 is different from that of x^2 by human supervision, then end the algorithm and return feature extractor $\Phi^* = \Phi^* \Phi'$ and classifier w^* , otherwise set $\Phi' = V_2^T \Phi'$, and update the environment data variable $X^e = V_2^T X^e$ for each e and then go to the **Step 1**.

Theorem 5 (Guarantee of CSIB). Suppose each $e \in \mathcal{E}_{all}$ follows Assumption 1 or 7 with S the orthogonal (invertible) transformation. Assume that the invariant features are strictly separable (5), bounded (Assumptions 2), and satisfy Assumptions 6. Also, for each $e \in \mathcal{E}_{tr}$ in Assumption 1, $Z_{spu}^e \leftarrow AZ_{inv}^e + W^e$ with $A \in \mathbb{R}^{o \times m}$ and $W^e \in \mathbb{R}^o$ or $Z_{inv}^e \leftarrow AZ_{spu}^e + W^e$ with $A \in \mathbb{R}^{m \times o}$ and $W^e \in \mathbb{R}^m$, where W^e is continuous (or discrete variable with each component at least two distinct values), bounded, and zero mean. Each solution to CSIB with l as 0-1 loss, $c \geq m$, and $r^{th} = q$ solves the OOD generalization (Eq. 1).

Significance of Theorem 5. CSIB succeeds without assuming the support overlap for invariant features and can apply to multiple cases where IB-IRM (as well as ERM, IRM, and IB-ERM) could fail by only requiring a single sample by further supervision. By such counterfactual intervention, CSIB works even when accessing data from a single environment, which is significant especially in the cases where multiple environmental data are not available.

4 Experiments

Following the motivating Examples, we perform experiments on three synthetic datasets from both the FIIF and PIIF cases to verify our method – counterfactual supervision-based information bottleneck (CSIB) – and compare it to ERM, IB-ERM, IRM, and IB-IRM. We follow the same protocol for tuning hyperparameters from [3, 4, 1] and report the classification error for all experiments. In the following, we first briefly describe the designed datasets and then report the main results. More experimental details can be found in Appendix.

4.1 Datasets

Example 1/1S (FIIF). The example is a modified one from the linear unit tests introduced in [4], which generalizes the cow/camel classification task with relevant backgrounds.

$$\begin{aligned}\theta_{cow} &= \mathbf{1}_m, & \theta_{camel} &= -\theta_{cow}, & \nu_{animal} &= 10^{-2} \\ \theta_{grass} &= \mathbf{1}_o, & \theta_{sand} &= -\theta_{grass}, & \nu_{background} &= 1.\end{aligned}$$

The dataset D_e of each environment $e \in \mathcal{E}_{all}$ is sampled from the following distribution

$$\begin{aligned}U^e &\sim \text{Categorical}(p^e s^e, (1-p^e)s^e, p^e(1-s^e), (1-p^e)(1-s^e)), \\ Z_{inv}^e &\sim \begin{cases} (\mathcal{N}_m(0, 0.1) + \theta_{cow})\nu_{animal} & \text{if } U^e \in \{1, 2\}, \\ (\mathcal{N}_m(0, 0.1) + \theta_{camel})\nu_{animal} & \text{if } U^e \in \{3, 4\}, \end{cases} \\ Z_{inv}^e &\sim \begin{cases} (\mathcal{N}_o(0, 0.1) + \theta_{grass})\nu_{background} & \text{if } U^e \in \{1, 4\}, \\ (\mathcal{N}_o(0, 0.1) + \theta_{sand})\nu_{background} & \text{if } U^e \in \{2, 3\}, \end{cases} \\ Z^e &\leftarrow (Z_{inv}^e, Z_{spu}^e), \quad X^e \leftarrow S(Z^e), \quad N^e \sim \text{Bernoulli}(q), \quad q < 0.5, \quad Y^e \leftarrow \mathbf{1}(\mathbf{1}_m^T Z_{inv}^e) \oplus N^e\end{aligned}$$

We set $s^{e_0} = 0.5$, $s^{e_1} = 0.7$, $s^{e_2} = 0.3$ for the first three environments, and $s^{e_j} \sim \text{Uniform}(0.3, 0.7)$ for $j > 3$. The scrambling matrix S is an identical matrix in Example 1 and a random unitary matrix in Example 1S. Here, we set $p^e = 1$ and $q = 0$ for all environments to make the spurious features and the

Table 1: Summary of three datasets. Note that for linearly separable features, their margin levels significantly influence the final learning classifier due to the implicit bias of the gradient descent [44]. Such bias would push the standard learning focusing more on the large-margin features.

Datasets	Margin relationship	Entropy relationship	Dim _{inv}	Dim _{spu}	Setting
Example 1/1S	Margin _{inv} \ll Margin _{spu}	Entropy _{inv} $<$ Entropy _{spu}	5	5	FIIF
Example 2/2S	Margin _{inv} \approx Margin _{spu}	Entropy _{inv} $>$ Entropy _{spu}	5	5	FIIF
Example 3/3S	Margin _{inv} \gg Margin _{spu}	Entropy _{inv} $>$ Entropy _{spu}	5	5	PIIF

invariant features both linearly separable to confuse each other. For the experiments on different values of q and p^e are presented in Appendix, where we have found very interesting observations related to the inductive bias of neural networks.

Example 2/2S (FIIF). This example is extended from the Example 2 to show one of the failure cases of IB-IRM (as well as ERM, IRM, and IB-ERM) and how our method can be improved by intervention. Given $w^e \in \mathbb{R}$, each instance in the environment data D^e is sampled by

$$\begin{aligned}\theta_{spu} &= 5 \cdot \mathbf{1}_o, \quad \theta_w = w^e \cdot \mathbf{1}_m, \quad \nu_{spu} = 10^{-2}, \quad \nu_w = 1, \quad p, q \sim \text{Bernoulli}(0.5), \\ Z_{spu}^e &= \mathcal{N}_o(0, 1)\nu_{spu} + (2p - 1) \cdot \theta_{spu}, \quad W^e = \mathcal{N}_m(0, 1)\nu_w + (2q - 1) \cdot \theta_w \\ Z_{inv}^e &= AZ_{spu}^e + W^e, \quad Z^e \leftarrow (Z_{inv}^e, Z_{spu}^e), \quad X^e \leftarrow S(Z^e), \quad Y^e = \mathbf{1}(\mathbf{1}_m^T Z_{inv}^e),\end{aligned}$$

where we set $m = o = 5$ and $A \in \mathbb{R}^{m \times o}$ be the identical matrix in our experiments. We set $w^{e_0} = 3$, $w^{e_1} = 2$, $w^{e_2} = 1$, and $w^{e_j} = \text{Uniform}(0, 3)$ if $j > 3$ for different training environments. This example shows clear smaller entropy of spurious features than that of invariant features, which is opposite to the Example 1/1S.

Example 3/3S (PIIF). This example extends from the Example 3 and similar to the construction of Example 2/2S but in the PIIF setting. Let $w^e \sim \text{Uniform}(0, 1)$ for different training environments. Each instance in the environments e is sampled by

$$\begin{aligned}\theta_{inv} &= 10 \cdot \mathbf{1}_m, \quad \nu_{inv} = 10, \quad \nu_{spu} = 1, \quad p, q \sim \text{Bernoulli}(0.5), \\ Z_{inv}^e &= \mathcal{N}_m(0, 1)\nu_{inv} + (2p - 1) \cdot \theta_{inv}, \quad Y^e = \mathbf{1}(\mathbf{1}_m^T Z_{inv}^e), \\ Z_{spu}^e &= 2(Y^e - 1) \cdot \nu_{spu} + (2q - 1) \cdot w^e \cdot \mathbf{1}_o, \quad Z^e \leftarrow (Z_{inv}^e, Z_{spu}^e), \quad X^e \leftarrow S(Z^e),\end{aligned}$$

where we set $m = o = 5$ in our experiments. The spurious features have smaller entropy than the invariant features in this example, which is similar to Example 2/2S, but the invariant features significantly enjoy much larger margin than the spurious features, which is very different from the above two examples. We make a summary to the properties of these three datasets in Table 1 for a general view.

4.2 Summary of results

Table 2 shows the classification errors of different methods when training data comes from single, three, and six environments. We can see that ERM and IRM fail to recognize the invariant features in the experiment of Example 1/1S, where invariant features have smaller margin than spurious features do, while information bottleneck-based methods (IB-ERM, IB-IRM, and CSIB) show improved results due to the smaller entropy of the invariant features. Our method CSIB shows consistent results with IB-IRM in Example 1/1S when invariant features are extracted in the first run, which verifies the effectiveness of information bottleneck for invariant feature learning in this case. In another FIIF setting of Example 2/2S, where the invariant features have larger entropy than spurious features do, we can see that only CSIB can remove the spurious features out among all comparing methods, although information bottleneck-based method IB-ERM would degrade the performance of ERM by focusing more on the spurious features. In the third experiments of Example 3/3S of PIIF setting, we can see that although ERM shows not-bad results due to the significantly larger margin of invariant features, our method CSIB still shows improvements by removing out more spurious features. Notably, comparing to the IB-ERM and IB-IRM when only spurious features are extracted (Example 2/2S, Example 3/3S), our

Table 2: Main results. #Envs means the number of training environments, and (min) reports the minimal test classification error across different running seeds.

	#Envs	ERM (min)	IRM (min)	IB-ERM (min)	IB-IRM (min)	CSIB (min)
Example 1	1	0.50 \pm 0.01 (0.49)	0.50 \pm 0.01 (0.49)	0.23 \pm 0.02 (0.22)	0.31 \pm 0.10 (0.25)	0.23 \pm 0.02 (0.22)
Example 1S	1	0.50 \pm 0.00 (0.49)	0.50 \pm 0.00 (0.50)	0.46 \pm 0.04 (0.39)	0.30 \pm 0.10 (0.25)	0.46 \pm 0.04 (0.39)
Example 2	1	0.40 \pm 0.20 (0.00)	0.50 \pm 0.00 (0.49)	0.50 \pm 0.00 (0.49)	0.46 \pm 0.02 (0.45)	0.00 \pm 0.00 (0.00)
Example 2S	1	0.50 \pm 0.00 (0.50)	0.31 \pm 0.23 (0.00)	0.50 \pm 0.00 (0.50)	0.45 \pm 0.01 (0.43)	0.10 \pm 0.20 (0.00)
Example 3	1	0.16 \pm 0.06 (0.09)	0.18 \pm 0.03 (0.14)	0.50 \pm 0.01 (0.49)	0.40 \pm 0.20 (0.01)	0.11 \pm 0.20 (0.00)
Example 3S	1	0.17 \pm 0.07 (0.10)	0.09 \pm 0.02 (0.07)	0.50 \pm 0.00 (0.50)	0.50 \pm 0.00 (0.50)	0.21 \pm 0.24 (0.00)
Example 1	3	0.45 \pm 0.01 (0.45)	0.45 \pm 0.01 (0.45)	0.22 \pm 0.01 (0.21)	0.23 \pm 0.13 (0.02)	0.22 \pm 0.01 (0.21)
Example 1S	3	0.45 \pm 0.00 (0.45)	0.45 \pm 0.00 (0.45)	0.41 \pm 0.04 (0.34)	0.27 \pm 0.11 (0.11)	0.41 \pm 0.04 (0.34)
Example 2	3	0.40 \pm 0.20 (0.00)	0.50 \pm 0.00 (0.50)	0.50 \pm 0.00 (0.50)	0.33 \pm 0.04 (0.25)	0.00 \pm 0.00 (0.00)
Example 2S	3	0.50 \pm 0.00 (0.50)	0.37 \pm 0.15 (0.15)	0.50 \pm 0.00 (0.50)	0.34 \pm 0.01 (0.33)	0.10 \pm 0.20 (0.00)
Example 3	3	0.18 \pm 0.04 (0.15)	0.21 \pm 0.02 (0.20)	0.50 \pm 0.01 (0.49)	0.50 \pm 0.01 (0.49)	0.11 \pm 0.20 (0.00)
Example 3S	3	0.18 \pm 0.04 (0.15)	0.08 \pm 0.03 (0.03)	0.50 \pm 0.00 (0.50)	0.43 \pm 0.09 (0.31)	0.01 \pm 0.00 (0.00)
Example 1	6	0.46 \pm 0.01 (0.44)	0.46 \pm 0.09 (0.41)	0.22 \pm 0.01 (0.20)	0.37 \pm 0.14 (0.17)	0.22 \pm 0.01 (0.20)
Example 1S	6	0.46 \pm 0.02 (0.44)	0.46 \pm 0.02 (0.44)	0.35 \pm 0.10 (0.23)	0.42 \pm 0.12 (0.28)	0.35 \pm 0.10 (0.23)
Example 2	6	0.49 \pm 0.01 (0.48)	0.50 \pm 0.01 (0.48)	0.50 \pm 0.00 (0.50)	0.30 \pm 0.01 (0.28)	0.00 \pm 0.00 (0.00)
Example 2S	6	0.50 \pm 0.00 (0.50)	0.35 \pm 0.12 (0.25)	0.50 \pm 0.00 (0.50)	0.30 \pm 0.01 (0.29)	0.20 \pm 0.24 (0.00)
Example 3	6	0.18 \pm 0.04 (0.15)	0.20 \pm 0.01 (0.19)	0.50 \pm 0.00 (0.49)	0.37 \pm 0.16 (0.16)	0.01 \pm 0.01 (0.00)
Example 3S	6	0.18 \pm 0.04 (0.14)	0.05 \pm 0.04 (0.01)	0.50 \pm 0.00 (0.50)	0.50 \pm 0.00 (0.50)	0.11 \pm 0.20 (0.00)

method CSIB could effectively remove them by intervention and then refocus on the invariant features. Note that the reason of non-zero average error and the fluctuant results of CSIB in some experiments is because the entropy minimization in the training process is less accurate, where entropy is substituted by variance for the ease of the optimization. Nevertheless, there always exists a case where the entropy is indeed truly minimized and the error reaches zero (see (min) in the table) in Example 2/2S and Example 3/3S. In summary, CSIB improves others consistently in both FIIF and PIIF settings and are especially more effective than IB-ERM and IB-IRM when the spurious features enjoy much smaller entropy than the invariant features do.

5 Related works

We divide the works related to OOD generalization into two categories: theory and methods, though some of them belong to both.

5.1 Theory of OOD generalization

Based on different definitions to the distributional changes, we review the corresponding theory by the following three categories.

Based on causality. Due to the close connection between the distributional changes and the interventions discussed in the theory of causality [34, 36], the problem of OOD generalization is usually built in the framework of causal learning. The theory states that a response Y is directly caused only by its parents variables $X_{Pa(Y)}$ and all interventions other than those on Y do not change the conditional distribution of $\mathbb{P}(Y|X_{Pa(Y)})$. Such theory inspires a popular learning principle – invariance principle – that aims to discover a set of variables such that they remain invariance to the response Y in all observed environments [35, 18, 39]. Invariant risk minimization (IRM) [3] is then proposed to learn a feature extractor Φ in an end-to-end way such that the classifier learned based on the extracted features $\Phi(X)$ remains unchange in each environment. The theory in [3] shows the guarantee of IRM for OOD generalization under some general assumptions, but only focuses on the linear regression tasks. Different from the failure analyses of IRM for the classification tasks in [41, 20] in the PIIF setting, Ahuja et al., [1] first show that under the FIIF setting, linear classification is more difficult than linear regression, where invariance principle itself is insufficient to ensure the success of OOD generalization, and claim that the assumption of support overlap of invariant features is necessarily needed. They then propose a learning principle of information bottleneck-based invariant risk minimization (IB-IRM) for linear classification, which shows how to address the failures of IRM by adding information bottleneck [47]

into the learning. In this work, we closely investigate the conditions identified in [1] and first show that support overlap of invariant features is not necessarily needed for the success of OOD generalization. We further show several failure cases of IB-IRM and propose improved results to it.

Recently, some of works are proposed to tackle the challenge of OOD generalization in the non-linear regime [28, 26]. Commonly, both of them use variational auto encoder (VAE)-based models [21, 38] to identify the latent variables from observations in the first stage. Then, these inferring latent variables are separated to two distinct parts of invariant (causal) and spurious (non-causal) features based on different assumptions on them. Specifically, Lu et al. [27, 28] assume that the latent variables conditioned on some accessible side information such as the environment index or class label are followed the exponential family distributions, and Liu et al. [26] directly disentangle the latent variables to two different parts during the inferring stage and assumes that the marginal distributions of them are independent to each other. These assumptions, however, are rather strong in general. Nevertheless, these solutions aim to capture the latent variables such that the response given these variables is invariant for different environments, which could still fail in the FIIF setting where the invariance principle itself is insufficient for OOD generalization in the classification tasks, as shown in [1]. In this work, we focus on the linear classification only and show a new theory of a new method that well addresses most of the OOD generalization failures in both PIIF and FIIF settings.

Based on robustness. Different from those based on the causality, where different distributions are generated by a same causal graph and the goal is to discover causal features, the robustness based methods aim to protect the model against the potential distributional shifts within the uncertainty set, which is usually constrained by f-divergence [32] or Wasserstein distance [43]. This series of works are theoretically addressed by distributionally robust optimization (DRO) under a minimax framework [23, 12]. Recently, some of works tend to connect the connections between causality and robustness [10]. Although these works show less relevance to us, it is possible that a well-defined measure of distribution divergence could help to effectively extract causal features under the robustness framework. This would be an interesting avenue for future research.

Others. Some other works assume that the distributions (domains) are generated from a hyper-distribution and aims to minimize the average risk estimation error bound [9, 30, 11]. These works are often built based on the generalization theory under the independent and identically distributed (IID) assumption. And in [53], it does not make any assumption to the distributional changes, and only studies the learnability of OOD generalization in a general way. All of these theories can not cover the OOD generalization problem under a single training environment or domain.

5.2 Methods of OOD generalization

Based on invariance principle. Inspired from the invariance principle [35, 18], many methods are proposed by designing various loss to extract features to better satisfy the principle itself. IRMv1 [3] is the first objective to address this in an end-to-end way by adding a gradient penalty to the classifier. Following this work, Krueger et al. [22] suggest penalizing the variance of the risks, while Xie et al. [51] give the same objective but taking the square root of the variance. And many other alternatives could also be found [19, 29, 6]. It is clear that all of these methods aims to find an invariant predictor. Recently, Ahuja et al. [1] find that for classification problem, finding the invariant predictor is not enough to extract causal features since the features could include the spurious information to make the predictor invariant across training environments, and they propose IB-IRM to address such failure. Similar idea to IB-IRM could also be found in the work [24], where a different loss function is proposed to achieve the same purpose. More recently, Wang et al. [49] propose the similar ideas to ours but only tackle the situation when the invariant features have the same distribution among all environments. In this work, we further show that IB-IRM could still fail in several cases due to the model may only rely on spurious features to make the predictor invariance. We then propose counterfactual supervision-based information bottleneck (CSIB) method to address such failures and show improving results to the prior works.

Based on distribution matching. It is worth to note that there exist many works focused on learning domain invariant features representations [13, 25, 56]. Most of these works are inspired by the seminal theory of domain adaptation [8, 7]. The goal of these methods is to learn a feature extractor Φ such that the marginal distribution of $\mathbb{P}(\Phi(X))$ or the conditional distribution of $\mathbb{P}(\Phi(X)|Y)$ is invariant across different domains. This is different from the invariance principle, where the goal is to make $\mathbb{P}(Y|\Phi(X))$ (or $\mathbb{E}(Y|\Phi(X))$) invariant. We refer readers to the papers of [3, 55] for better understanding

the details of why these distribution matching based methods often fail to address OOD generalization.

Others. Other related methods are various, including by using data augmentation in both image level [52] or feature level [57], by removing spurious correlations through stable learning [54], and by utilizing the inductive bias of neural network [15, 48] etc. Most of these methods are empirically inspired from the experiments and are verified to some specific datasets. Recently, an empirical study in [16, 50] notices that the real effects of many OOD generalization (domain generalization) methods are weak, which indicates that the benchmark-based evaluation criterions may be inadequate to validate the OOD generalization algorithms.

6 Conclusion, limitations and future work

In this paper, we focus on the OOD generalization problem of linear classification. We first revisit the fundamental assumptions and results of prior works and show that the condition of invariant features support overlap is not necessarily needed for the success of OOD generalization and thus propose a weaker counterpart. Then, we show several failure cases of IB-IRM (as well as ERM, IB-ERM, and IRM) and illustrate its intrinsic causes by theoretical analysis. Motivating by that, we further propose a new method – counterfactual supervision-based information bottleneck (CSIB) and theoretically prove its effectiveness under some weaker assumptions. CSIB works even when accessing data from a single environment, and has theoretically consistent results for both binary and multi-class problems. Finally, we design several synthetic datasets by our motivating examples for the experimental verification. Empirical observations among all comparing methods illustrate the effectiveness of CSIB.

Since we only take the linear problem into interest, including linear representation and linear classifier, any non-linear case of that would not be guaranteed by our theoretical results and thus CSIB may fail. Therefore, the same as prior works (IRM [3] and IB-IRM [1]), non-linear challenge is still an unsolved problem [41, 20]. We believe this is of great value for investigating in future work since widely used data in the wild are non-linearly generated. Another fruitful direction is to design a powerful algorithm for entropy minimization during the learning process of CSIB. Currently, we use the variance of features to replace the entropy of the features during the optimization. However, variance and entropy are essentially different but a truly effective entropy minimization is the key to the success of CSIB. Another limitation of our method is that we have to require a further supervision to the counterfactual examples during the learning time, although it only takes one time for a single step.

References

- [1] Kartik Ahuja, Ethan Caballero, Dinghuai Zhang, Jean-Christophe Gagnon-Audet, Yoshua Bengio, Ioannis Mitliagkas, and Irina Rish. Invariance principle meets information bottleneck for out-of-distribution generalization. *Neural Information Processing Systems*, 34, 2021.
- [2] Kartik Ahuja, Karthikeyan Shanmugam, Kush Varshney, and Amit Dhurandhar. Invariant risk minimization games. In *International Conference on Machine Learning*, pages 145–155. PMLR, 2020.
- [3] Martin Arjovsky, Léon Bottou, Ishaan Gulrajani, and David Lopez-Paz. Invariant risk minimization. *arXiv preprint arXiv:1907.02893*, 2019.
- [4] Benjamin Aubin, Agnieszka Slowik, Martin Arjovsky, Leon Bottou, and David Lopez-Paz. Linear unit-tests for invariance discovery. *arXiv preprint arXiv:2102.10867*, 2021.
- [5] Sara Beery, Grant Van Horn, and Pietro Perona. Recognition in terra incognita. In *European Conference on Computer Vision*, pages 456–473, 2018.
- [6] Alexis Bellot and Mihaela van der Schaar. Generalization and invariances in the presence of unobserved confounding. *arXiv preprint arXiv:2007.10653*, 11, 2020.
- [7] Shai Ben-David, John Blitzer, Koby Crammer, Alex Kulesza, Fernando Pereira, and Jennifer Wortman Vaughan. A theory of learning from different domains. *Machine learning*, 79(1):151–175, 2010.

- [8] Shai Ben-David, John Blitzer, Koby Crammer, and Fernando Pereira. Analysis of representations for domain adaptation. *Advances in neural information processing systems*, 19, 2006.
- [9] Gilles Blanchard, Gyemin Lee, and Clayton Scott. Generalizing from several related classification tasks to a new unlabeled sample. *Advances in neural information processing systems*, 24, 2011.
- [10] Peter Bühlmann. Invariance, causality and robustness. *Statistical Science*, 35(3):404–426, 2020.
- [11] Aniket Anand Deshmukh, Yunwen Lei, Srinagesh Sharma, Urun Dogan, James W Cutler, and Clayton Scott. A generalization error bound for multi-class domain generalization. *arXiv preprint arXiv:1905.10392*, 2019.
- [12] John C Duchi and Hongseok Namkoong. Learning models with uniform performance via distributionally robust optimization. *The Annals of Statistics*, 49(3):1378–1406, 2021.
- [13] Yaroslav Ganin and Victor Lempitsky. Unsupervised domain adaptation by backpropagation. In *International conference on machine learning*, pages 1180–1189. PMLR, 2015.
- [14] Robert Geirhos, Jörn-Henrik Jacobsen, Claudio Michaelis, Richard Zemel, Wieland Brendel, Matthias Bethge, and Felix A Wichmann. Shortcut learning in deep neural networks. *Nature Machine Intelligence*, 2(11):665–673, 2020.
- [15] Robert Geirhos, Patricia Rubisch, Claudio Michaelis, Matthias Bethge, Felix A Wichmann, and Wieland Brendel. Imagenet-trained cnns are biased towards texture; increasing shape bias improves accuracy and robustness. In *International Conference on Learning Representations*, 2019.
- [16] Ishaan Gulrajani and David Lopez-Paz. In search of lost domain generalization. In *International Conference on Learning Representations*, 2020.
- [17] Suchin Gururangan, Swabha Swayamdipta, Omer Levy, Roy Schwartz, Samuel R Bowman, and Noah A Smith. Annotation artifacts in natural language inference data. In *NAACL-HLT (2)*, 2018.
- [18] Christina Heinze-Deml, Jonas Peters, and Nicolai Meinshausen. Invariant causal prediction for nonlinear models. *Journal of Causal Inference*, 6(2), 2018.
- [19] Wengong Jin, Regina Barzilay, and Tommi Jaakkola. Domain extrapolation via regret minimization. *arXiv preprint arXiv:2006.03908*, 2020.
- [20] Pritish Kamath, Akilesh Tangella, Danica Sutherland, and Nathan Srebro. Does invariant risk minimization capture invariance? In *International Conference on Artificial Intelligence and Statistics*, pages 4069–4077. PMLR, 2021.
- [21] Diederik P Kingma and Max Welling. Auto-encoding variational bayes. *arXiv preprint arXiv:1312.6114*, 2013.
- [22] David Krueger, Ethan Caballero, Joern-Henrik Jacobsen, Amy Zhang, Jonathan Binas, Dinghuai Zhang, Remi Le Priol, and Aaron Courville. Out-of-distribution generalization via risk extrapolation (rex). In *International Conference on Machine Learning*, pages 5815–5826. PMLR, 2021.
- [23] Jaeho Lee and Maxim Raginsky. Minimax statistical learning with wasserstein distances. *Advances in Neural Information Processing Systems*, 31, 2018.
- [24] Bo Li, Yifei Shen, Yezhen Wang, Wenzhen Zhu, Colorado J Reed, Jun Zhang, Dongsheng Li, Kurt Keutzer, and Han Zhao. Invariant information bottleneck for domain generalization. In *Association for the Advancement of Artificial Intelligence*, 2022.
- [25] Ya Li, Xinmei Tian, Mingming Gong, Yajing Liu, Tongliang Liu, Kun Zhang, and Dacheng Tao. Deep domain generalization via conditional invariant adversarial networks. In *Proceedings of the European Conference on Computer Vision (ECCV)*, pages 624–639, 2018.
- [26] Chang Liu, Xinwei Sun, Jindong Wang, Haoyue Tang, Tao Li, Tao Qin, Wei Chen, and Tie-Yan Liu. Learning causal semantic representation for out-of-distribution prediction. *Neural Information Processing Systems*, 34, 2021.

- [27] Chaochao Lu, Yuhuai Wu, José Miguel Hernández-Lobato, and Bernhard Schölkopf. Nonlinear invariant risk minimization: A causal approach. *arXiv preprint arXiv:2102.12353*, 2021.
- [28] Chaochao Lu, Yuhuai Wu, José Miguel Hernández-Lobato, and Bernhard Schölkopf. Invariant causal representation learning for out-of-distribution generalization. In *International Conference on Learning Representations*, 2022.
- [29] Divyat Mahajan, Shruti Tople, and Amit Sharma. Domain generalization using causal matching. In *International Conference on Machine Learning*, pages 7313–7324. PMLR, 2021.
- [30] Krikamol Muandet, David Balduzzi, and Bernhard Schölkopf. Domain generalization via invariant feature representation. In *International Conference on Machine Learning*, pages 10–18. PMLR, 2013.
- [31] Vaishnavh Nagarajan, Anders Andreassen, and Behnam Neyshabur. Understanding the failure modes of out-of-distribution generalization. In *International Conference on Learning Representations*, 2021.
- [32] Hongseok Namkoong and John C Duchi. Stochastic gradient methods for distributionally robust optimization with f-divergences. *Advances in neural information processing systems*, 29, 2016.
- [33] Anh Nguyen, Jason Yosinski, and Jeff Clune. Deep neural networks are easily fooled: High confidence predictions for unrecognizable images. In *Computer Vision and Pattern Recognition Conference*, pages 427–436, 2015.
- [34] Judea Pearl. *Causality*. Cambridge university press, 2009.
- [35] Jonas Peters, Peter Bühlmann, and Nicolai Meinshausen. Causal inference by using invariant prediction: identification and confidence intervals. *Journal of the Royal Statistical Society: Series B (Statistical Methodology)*, 78(5):947–1012, 2016.
- [36] Jonas Peters, Dominik Janzing, and Bernhard Schölkopf. *Elements of causal inference: foundations and learning algorithms*. The MIT Press, 2017.
- [37] Mohammad Pezeshki, Oumar Kaba, Yoshua Bengio, Aaron C Courville, Doina Precup, and Guillaume Lajoie. Gradient starvation: A learning proclivity in neural networks. *Neural Information Processing Systems*, 34, 2021.
- [38] Danilo Jimenez Rezende, Shakir Mohamed, and Daan Wierstra. Stochastic backpropagation and approximate inference in deep generative models. In *International Conference on Machine Learning*, pages 1278–1286. PMLR, 2014.
- [39] Mateo Rojas-Carulla, Bernhard Schölkopf, Richard Turner, and Jonas Peters. Invariant models for causal transfer learning. *The Journal of Machine Learning Research*, 19(1):1309–1342, 2018.
- [40] Amir Rosenfeld, Richard Zemel, and John K Tsotsos. The elephant in the room. *arXiv preprint arXiv:1808.03305*, 2018.
- [41] Elan Rosenfeld, Pradeep Kumar Ravikumar, and Andrej Risteski. The risks of invariant risk minimization. In *International Conference on Learning Representations*, 2021.
- [42] Shai Shalev-Shwartz and Shai Ben-David. *Understanding machine learning: From theory to algorithms*. Cambridge university press, 2014.
- [43] Aman Sinha, Hongseok Namkoong, Riccardo Volpi, and John Duchi. Certifying some distributional robustness with principled adversarial training. *arXiv preprint arXiv:1710.10571*, 2017.
- [44] Daniel Soudry, Elad Hoffer, Mor Shpigel Nacson, Suriya Gunasekar, and Nathan Srebro. The implicit bias of gradient descent on separable data. *The Journal of Machine Learning Research*, 19(1):2822–2878, 2018.
- [45] Christian Szegedy, Wojciech Zaremba, Ilya Sutskever, Joan Bruna, Dumitru Erhan, Ian Goodfellow, and Rob Fergus. Intriguing properties of neural networks. *arXiv preprint arXiv:1312.6199*, 2013.

- [46] MTCAJ Thomas and A Thomas Joy. *Elements of information theory*. Wiley-Interscience, 2006.
- [47] N TISHBY. The information bottleneck method. In *Proc. 37th Annual Allerton Conference on Communications, Control and Computing*, pages 368–377, 1999.
- [48] Haohan Wang, Songwei Ge, Zachary Lipton, and Eric P Xing. Learning robust global representations by penalizing local predictive power. In *Advances in Neural Information Processing Systems*, volume 32, 2019.
- [49] Haoxiang Wang, Haozhe Si, Bo Li, and Han Zhao. Provable domain generalization via invariant-feature subspace recovery. In *International Conference on Machine Learning*, 2022.
- [50] Olivia Wiles, Sven Gowal, Florian Stimberg, Sylvestre-Alvise Rebuffi, Ira Ktena, Krishnamurthy Dj Dvijotham, and Ali Taylan Cemgil. A fine-grained analysis on distribution shift. In *International Conference on Learning Representations*, 2022.
- [51] Chuanlong Xie, Fei Chen, Yue Liu, and Zhenguo Li. Risk variance penalization: From distributional robustness to causality. *arXiv preprint arXiv:2006.07544*, 1, 2020.
- [52] Qinwei Xu, Ruipeng Zhang, Ya Zhang, Yanfeng Wang, and Qi Tian. A fourier-based framework for domain generalization. In *Proceedings of the IEEE/CVF Conference on Computer Vision and Pattern Recognition*, pages 14383–14392, 2021.
- [53] Haotian Ye, Chuanlong Xie, Tianle Cai, Ruichen Li, Zhenguo Li, and Liwei Wang. Towards a theoretical framework of out-of-distribution generalization. In *Neural Information Processing Systems*, 2021.
- [54] Xingxuan Zhang, Peng Cui, Renzhe Xu, Linjun Zhou, Yue He, and Zheyang Shen. Deep stable learning for out-of-distribution generalization. In *Proceedings of the IEEE/CVF Conference on Computer Vision and Pattern Recognition*, pages 5372–5382, 2021.
- [55] Han Zhao, Remi Tachet Des Combes, Kun Zhang, and Geoffrey Gordon. On learning invariant representations for domain adaptation. In *International Conference on Machine Learning*, pages 7523–7532. PMLR, 2019.
- [56] Shanshan Zhao, Mingming Gong, Tongliang Liu, Huan Fu, and Dacheng Tao. Domain generalization via entropy regularization. *Advances in Neural Information Processing Systems*, 33:16096–16107, 2020.
- [57] Kaiyang Zhou, Yongxin Yang, Yu Qiao, and Tao Xiang. Domain generalization with mixstyle. In *International Conference on Learning Representations*, 2021.

A Appendix

A.1 Experiments details

In this section, we provide more details on the experiments. The code to reproduce the experiments can be found at <https://github.com/szubing/CSIB>.

A.1.1 Optimization loss of IB-ERM

The objective function of IB-ERM is as follow:

$$\min_{w, \Phi} \sum_{e \in \mathcal{E}_{tr}} h^e(\Phi) \quad \text{s.t.} \quad \frac{1}{|\mathcal{E}_{tr}|} \sum_{e \in \mathcal{E}_{tr}} R^e(w \cdot \Phi) \leq r^{th}. \quad (10)$$

Since the entropy of $h^e(\Phi) = H(\Phi(X^e))$ is hard to estimate by a differential variable that can be optimized by using gradient descent, we follow [1] by using the variance instead of the entropy for optimization. The total loss function is given by

$$loss(w, \Phi) = \sum_{e \in \mathcal{E}_{tr}} (R^e(w \cdot \Phi) + \lambda \text{Var}(\Phi)) \quad (11)$$

with a hyperparameter λ onto it.

A.1.2 Experiments setup

Model, hyperparameters, loss, and evaluation. In all experiments, we follow the same protocol as prescribed by [4, 1] for the model / hyperparameter selection, training, and evaluation. Except those specified, for all experiments across three Examples and five comparing methods, the model is the same with a linear feature extractor $\Phi \in \mathbb{R}^{d \times d}$ followed by a linear classifier $w \in \mathbb{R}^{d+1}$. We use binary cross-entropy loss for classification. All hyperparameters, including the learning rate, the penalty term in IRM, or the λ associated with the $\text{Var}(\Phi)$ in Eq. (11), etc., are randomly searched and selected by using 20 test samples for validation. The results reported in the main manuscript use 3 hyperparameter queries of each and average over 5 data seeds. The results when searching over more hyperparameter values are reported in the supplementary experiments. The search spaces of all the hyperparameters follow the same as in [4, 1]. The classification test errors between 0 and 1 are reported.

Compute description. Our computing resource is one GPU of NVIDIA GeForce GTX 1080 Ti with 6 CPU cores of Intel(R) Core(TM) i7-8700 CPU @ 3.20GHz.

Existing codes and datasets used. In our experiments, we mainly rely on the following two github repositories: InvarianceUnitTests² and IB-IRM³.

A.1.3 Supplementary experiments

The purpose of the first supplementary experiment is to illustrate what the result would be when we increase the number of running seeds in the hyperparameters selection. These results are shown in Tab. A1, where we increase the number of hyperparameter queries to 10 of each. It is clear that in overall, the results of CSIB in Tab. A1 are much better and have less fluctuations than those in Tab. 2, and the conclusions remain almost the same as we have summarized in section 4.2. This further verifies the effectiveness of CSIB method.

Observation on different settings in Example 1/1S. In our main experiments of Example 1/1S, we set $p^e = 1$ and $q = 0$ to make the spurious features and the invariant features both linearly separable to confuse each other. Here, we analyse what the result would be if we vary the values of them. Following [4], we set $p^{e_0} = 0.95$, $p^{e_1} = 0.97$, $p^{e_2} = 0.99$, and $p^{e_j} \sim \text{Uniform}(0.9, 1)$ to make spurious features linearly inseparable, and q is set to 0/0.05 to make invariant features linearly separable/inseparable. Tab. A2 shows the corresponding results. Interestingly, we find that all methods except for IB-IRM have ideal error rate (the same as the Oracle) when the spurious features are linearly inseparable ($p^e \neq 1$), even when the invariant features are linearly inseparable too ($q = 0.05$). Why would this happen? We then remove the linear embedding Φ , the results are presented in Tab. A3.

²<https://github.com/facebookresearch/InvarianceUnitTests>

³<https://github.com/ahujak/IB-IRM>

Table A1: Supplementary results when using 10 hyperparameter queries. #Envs means the number of training environments, and (min) reports the minimal test classification error across different running data seeds.

	#Envs	ERM (min)	IRM (min)	IB-ERM (min)	IB-IRM (min)	CSIB (min)	Oracle (min)
Example 1	1	0.50 ± 0.01 (0.49)	0.50 ± 0.01 (0.49)	0.23 ± 0.02 (0.22)	0.31 ± 0.10 (0.25)	0.23 ± 0.02 (0.22)	0.00 ± 0.00 (0.00)
Example 1S	1	0.50 ± 0.00 (0.49)	0.50 ± 0.00 (0.49)	0.09 ± 0.04 (0.04)	0.30 ± 0.10 (0.25)	0.08 ± 0.04 (0.04)	0.00 ± 0.00 (0.00)
Example 2	1	0.40 ± 0.20 (0.00)	0.00 ± 0.00 (0.00)	0.50 ± 0.00 (0.49)	0.48 ± 0.03 (0.43)	0.00 ± 0.00 (0.00)	0.00 ± 0.00 (0.00)
Example 2S	1	0.50 ± 0.00 (0.50)	0.30 ± 0.25 (0.00)	0.50 ± 0.00 (0.50)	0.50 ± 0.01 (0.48)	0.00 ± 0.00 (0.00)	0.00 ± 0.00 (0.00)
Example 3	1	0.16 ± 0.06 (0.09)	0.03 ± 0.00 (0.03)	0.50 ± 0.01 (0.49)	0.41 ± 0.09 (0.25)	0.02 ± 0.01 (0.00)	0.00 ± 0.00 (0.00)
Example 3S	1	0.16 ± 0.06 (0.10)	0.04 ± 0.01 (0.02)	0.50 ± 0.00 (0.50)	0.41 ± 0.12 (0.26)	0.01 ± 0.01 (0.00)	0.00 ± 0.00 (0.00)
Example 1	3	0.44 ± 0.01 (0.44)	0.44 ± 0.01 (0.44)	0.21 ± 0.00 (0.21)	0.21 ± 0.10 (0.06)	0.21 ± 0.00 (0.21)	0.00 ± 0.00 (0.00)
Example 1S	3	0.45 ± 0.00 (0.44)	0.45 ± 0.00 (0.44)	0.09 ± 0.03 (0.05)	0.23 ± 0.13 (0.01)	0.09 ± 0.03 (0.05)	0.00 ± 0.00 (0.00)
Example 2	3	0.13 ± 0.07 (0.00)	0.00 ± 0.00 (0.00)	0.50 ± 0.00 (0.50)	0.33 ± 0.04 (0.25)	0.00 ± 0.00 (0.00)	0.00 ± 0.00 (0.00)
Example 2S	3	0.50 ± 0.00 (0.50)	0.14 ± 0.20 (0.00)	0.50 ± 0.00 (0.50)	0.34 ± 0.01 (0.33)	0.00 ± 0.00 (0.00)	0.00 ± 0.00 (0.00)
Example 3	3	0.17 ± 0.04 (0.14)	0.02 ± 0.00 (0.02)	0.50 ± 0.01 (0.49)	0.43 ± 0.08 (0.29)	0.01 ± 0.00 (0.00)	0.00 ± 0.00 (0.00)
Example 3S	3	0.17 ± 0.04 (0.13)	0.02 ± 0.00 (0.02)	0.50 ± 0.00 (0.50)	0.36 ± 0.18 (0.07)	0.01 ± 0.00 (0.00)	0.00 ± 0.00 (0.00)
Example 1	6	0.46 ± 0.01 (0.44)	0.46 ± 0.09 (0.41)	0.22 ± 0.01 (0.21)	0.41 ± 0.11 (0.26)	0.22 ± 0.01 (0.21)	0.00 ± 0.00 (0.00)
Example 1S	6	0.46 ± 0.02 (0.44)	0.46 ± 0.02 (0.44)	0.06 ± 0.04 (0.02)	0.45 ± 0.07 (0.41)	0.06 ± 0.04 (0.02)	0.00 ± 0.00 (0.00)
Example 2	6	0.21 ± 0.03 (0.17)	0.00 ± 0.00 (0.00)	0.50 ± 0.00 (0.50)	0.36 ± 0.03 (0.31)	0.00 ± 0.00 (0.00)	0.00 ± 0.00 (0.00)
Example 2S	6	0.50 ± 0.00 (0.50)	0.10 ± 0.20 (0.00)	0.50 ± 0.00 (0.50)	0.19 ± 0.16 (0.01)	0.00 ± 0.00 (0.00)	0.00 ± 0.00 (0.00)
Example 3	6	0.17 ± 0.03 (0.14)	0.02 ± 0.00 (0.02)	0.50 ± 0.00 (0.49)	0.37 ± 0.16 (0.16)	0.01 ± 0.00 (0.00)	0.00 ± 0.00 (0.00)
Example 3S	6	0.17 ± 0.03 (0.14)	0.02 ± 0.00 (0.02)	0.50 ± 0.00 (0.50)	0.46 ± 0.09 (0.28)	0.01 ± 0.00 (0.00)	0.00 ± 0.00 (0.00)

Comparing the results between Tables A2 and A3, we found there is a significant inductive bias of neural network, though the model is linear. Further analysis to such observation is out of scope of this paper, but this would be an interesting avenue for future research.

Observation on linearly separable properties of high-dimensional data. In here, we empirically show that for o -dimensional data, we have high probability that o randomly drawn points are linearly separable for any two subsets. To verify that, we design a random experiment as follows: (1) Let $o \in [100, 10000]$, and we randomly drawn o points from $[-1, 1]^o$, and give random labels to these o points of 0 or 1; (2) We train a linear classifier to fit these o points and report the final training error; (3) Do (1) and (2) 100 times for different seeds. Our results show that for 100 runs, all training errors reach to 0 for every o , which proves our conjecture.

Then, we look back to the Theorem 4. For real data like image, the dimension of spurious features o is often high. Assume different environments enjoy different spurious points randomly, then from the above observation, there is a high probability that the following events will occur: For any labeling data in the n training environments with $n < o/2$ (2 is due to binary label), models could achieve zero training error by relying on spurious features only. This illustrates why prior methods easily fail to address OOD generalization in Assumption 7.

A.2 Proofs

A.2.1 Preliminary

Before our proofs, we first review some useful properties related to the entropy [46, 1].

Entropy. For discrete random variable $X \sim \mathbb{P}_X$ with support \mathcal{X} , its entropy (Shannon entropy) is defined as

$$H(X) = - \sum_{x \in \mathcal{X}} \mathbb{P}_X(X = x) \log(\mathbb{P}_X(X = x)) \quad (12)$$

The differential entropy of the continuous random variable $X \sim \mathbb{P}_X$ with support \mathcal{X} is given by

$$h(X) = - \int_{x \in \mathcal{X}} p_X(x) \log(p_X(x)) dx, \quad (13)$$

where $p_X(x)$ is the probability density function of the distribution \mathbb{P}_X . Sometimes we may confuse using $H(X)$ or $h(X)$ to represent its entropy no matter X is discrete or continuous.

Lemma A.1. *If X and Y are discrete random variables that are independent, then*

$$H(X + Y) \geq \max\{H(X), H(Y)\}. \quad (14)$$

Table A2: Results in Example 1/1S, where the learning model is a linear embedding $\Phi \in \mathbb{R}^{d \times d}$ followed by a linear classifier $w \in \mathbb{R}^{d+1}$.

	#Envs	$p^e = 1?$	q	ERM	IB-ERM	IB-IRM	CSIB	IRM	Oracle
Example 1	1	Yes	0	0.50 \pm 0.01	0.23 \pm 0.02	0.31 \pm 0.10	0.23 \pm 0.02	0.50 \pm 0.01	0.00 \pm 0.00
Example 1S	1	Yes	0	0.50 \pm 0.00	0.46 \pm 0.04	0.30 \pm 0.10	0.46 \pm 0.04	0.50 \pm 0.00	0.00 \pm 0.00
Example 1	3	Yes	0	0.45 \pm 0.01	0.22 \pm 0.01	0.23 \pm 0.13	0.22 \pm 0.01	0.45 \pm 0.01	0.00 \pm 0.00
Example 1S	3	Yes	0	0.45 \pm 0.00	0.41 \pm 0.04	0.27 \pm 0.11	0.41 \pm 0.04	0.45 \pm 0.00	0.00 \pm 0.00
Example 1	6	Yes	0	0.46 \pm 0.01	0.22 \pm 0.01	0.37 \pm 0.14	0.22 \pm 0.01	0.46 \pm 0.09	0.00 \pm 0.00
Example 1S	6	Yes	0	0.46 \pm 0.02	0.35 \pm 0.10	0.42 \pm 0.12	0.35 \pm 0.10	0.46 \pm 0.02	0.00 \pm 0.00
Example 1	1	No	0	0.00 \pm 0.00	0.00 \pm 0.00	0.15 \pm 0.20	0.00 \pm 0.00	0.00 \pm 0.00	0.00 \pm 0.00
Example 1S	1	No	0	0.00 \pm 0.00	0.00 \pm 0.00	0.12 \pm 0.19	0.00 \pm 0.00	0.00 \pm 0.00	0.00 \pm 0.00
Example 1	3	No	0	0.00 \pm 0.00	0.00 \pm 0.00	0.00 \pm 0.00	0.00 \pm 0.00	0.00 \pm 0.00	0.00 \pm 0.00
Example 1S	3	No	0	0.00 \pm 0.00	0.00 \pm 0.00	0.00 \pm 0.01	0.00 \pm 0.00	0.00 \pm 0.00	0.00 \pm 0.00
Example 1	6	No	0	0.00 \pm 0.00	0.00 \pm 0.00	0.30 \pm 0.20	0.00 \pm 0.00	0.00 \pm 0.00	0.00 \pm 0.00
Example 1S	6	No	0	0.00 \pm 0.00	0.00 \pm 0.00	0.31 \pm 0.20	0.00 \pm 0.00	0.04 \pm 0.06	0.00 \pm 0.00
Example 1	1	No	0.05	0.05 \pm 0.00	0.05 \pm 0.00	0.32 \pm 0.22	0.05 \pm 0.00	0.05 \pm 0.00	0.05 \pm 0.00
Example 1S	1	No	0.05	0.05 \pm 0.00	0.05 \pm 0.00	0.19 \pm 0.17	0.05 \pm 0.00	0.05 \pm 0.00	0.05 \pm 0.00
Example 1	3	No	0.05	0.05 \pm 0.00	0.05 \pm 0.00	0.07 \pm 0.03	0.05 \pm 0.00	0.05 \pm 0.00	0.05 \pm 0.00
Example 1S	3	No	0.05	0.05 \pm 0.00	0.05 \pm 0.00	0.05 \pm 0.00	0.05 \pm 0.00	0.05 \pm 0.00	0.05 \pm 0.00
Example 1	6	No	0.05	0.05 \pm 0.00	0.05 \pm 0.00	0.30 \pm 0.21	0.05 \pm 0.00	0.05 \pm 0.00	0.05 \pm 0.00
Example 1S	6	No	0.05	0.05 \pm 0.00	0.05 \pm 0.00	0.32 \pm 0.19	0.05 \pm 0.00	0.05 \pm 0.00	0.05 \pm 0.00

Table A3: Results in Example 1/1S, where the learning model is a linear classifier $w \in \mathbb{R}^{d+1}$ without linear embedding Φ . CSIB must requires a feature extractor, so there are not results related to CSIB.

	#Envs	$p^e = 1?$	q	ERM	IB-ERM	IB-IRM	IRM	Oracle
Example 1	1	Yes	0	0.50 \pm 0.01	0.25 \pm 0.01	0.31 \pm 0.10	0.50 \pm 0.01	0.00 \pm 0.00
Example 1S	1	Yes	0	0.50 \pm 0.00	0.49 \pm 0.01	0.30 \pm 0.10	0.50 \pm 0.00	0.00 \pm 0.00
Example 1	3	Yes	0	0.44 \pm 0.01	0.23 \pm 0.01	0.21 \pm 0.10	0.44 \pm 0.01	0.00 \pm 0.00
Example 1S	3	Yes	0	0.45 \pm 0.00	0.44 \pm 0.01	0.42 \pm 0.04	0.45 \pm 0.00	0.00 \pm 0.00
Example 1	6	Yes	0	0.46 \pm 0.01	0.27 \pm 0.07	0.41 \pm 0.11	0.46 \pm 0.01	0.01 \pm 0.01
Example 1S	6	Yes	0	0.46 \pm 0.02	0.42 \pm 0.08	0.46 \pm 0.09	0.46 \pm 0.02	0.01 \pm 0.02
Example 1	1	No	0	0.50 \pm 0.01	0.00 \pm 0.00	0.15 \pm 0.20	0.50 \pm 0.01	0.00 \pm 0.00
Example 1S	1	No	0	0.50 \pm 0.00	0.00 \pm 0.00	0.13 \pm 0.19	0.50 \pm 0.00	0.00 \pm 0.00
Example 1	3	No	0	0.45 \pm 0.01	0.00 \pm 0.00	0.00 \pm 0.00	0.45 \pm 0.01	0.00 \pm 0.00
Example 1S	3	No	0	0.45 \pm 0.00	0.01 \pm 0.02	0.08 \pm 0.14	0.46 \pm 0.02	0.00 \pm 0.00
Example 1	6	No	0	0.46 \pm 0.01	0.10 \pm 0.16	0.30 \pm 0.20	0.46 \pm 0.01	0.01 \pm 0.01
Example 1S	6	No	0	0.46 \pm 0.01	0.24 \pm 0.19	0.41 \pm 0.12	0.47 \pm 0.03	0.01 \pm 0.02
Example 1	1	No	0.05	0.50 \pm 0.01	0.05 \pm 0.00	0.32 \pm 0.22	0.50 \pm 0.01	0.05 \pm 0.00
Example 1S	1	No	0.05	0.50 \pm 0.01	0.05 \pm 0.01	0.20 \pm 0.17	0.50 \pm 0.00	0.05 \pm 0.00
Example 1	3	No	0.05	0.45 \pm 0.01	0.05 \pm 0.00	0.07 \pm 0.03	0.47 \pm 0.01	0.05 \pm 0.00
Example 1S	3	No	0.05	0.45 \pm 0.01	0.07 \pm 0.03	0.11 \pm 0.11	0.46 \pm 0.01	0.05 \pm 0.00
Example 1	6	No	0.05	0.47 \pm 0.01	0.14 \pm 0.14	0.30 \pm 0.21	0.47 \pm 0.01	0.05 \pm 0.00
Example 1S	6	No	0.05	0.47 \pm 0.01	0.27 \pm 0.18	0.42 \pm 0.11	0.47 \pm 0.01	0.05 \pm 0.01

Proof. Define $Z = X + Y$. Since $X \perp Y$, we have

$$\begin{aligned}
H(Z|X) &= - \sum_{x \in \mathcal{X}} \mathbb{P}_X(x) \sum_{z \in \mathcal{Z}} \mathbb{P}_{Z|X}(Z = z|X = x) \log(\mathbb{P}_{Z|X}(Z = z|X = x)) \\
&= - \sum_{x \in \mathcal{X}} \mathbb{P}_X(x) \sum_{z \in \mathcal{Z}} \mathbb{P}_{Y|X}(Y = z - x|X = x) \log(\mathbb{P}_{Y|X}(Y = z - x|X = x)) \\
&= - \sum_{x \in \mathcal{X}} \mathbb{P}_X(x) \sum_{z \in \mathcal{Z}} \mathbb{P}_Y(Y = z - x) \log(\mathbb{P}_Y(Y = z - x)) \\
&= - \sum_{x \in \mathcal{X}} \mathbb{P}_X(x) \sum_{y \in \mathcal{Y}} \mathbb{P}_Y(Y = y) \log(\mathbb{P}_Y(Y = y)) \\
&= H(Y),
\end{aligned}$$

and similar we have $H(Z|Y) = H(X)$. Therefore,

$$H(X + Y) = I(Z, X) + H(Z|X) = I(Z, X) + H(Y) \geq H(Y) \quad (15)$$

$$H(X + Y) = I(Z, Y) + H(Z|Y) = I(Z, Y) + H(X) \geq H(X). \quad (16)$$

This completes the proof. \square

Lemma A.2. *If X and Y are continuous random variables that are independent, then*

$$h(X + Y) \geq \max\{h(X), h(Y)\}. \quad (17)$$

Proof. Define $Z = X + Y$. Since $X \perp Y$, we have

$$\begin{aligned}
h(Z|X) &= - \int_{x \in \mathcal{X}} p_X(x) \int_{z \in \mathcal{Z}} p_{Z|X}(Z = z|X = x) \log(p_{Z|X}(Z = z|X = x)) dx dz \\
&= - \int_{x \in \mathcal{X}} p_X(x) \int_{z \in \mathcal{Z}} p_{Y|X}(Y = z - x|X = x) \log(p_{Y|X}(Y = z - x|X = x)) dx dz \\
&= - \int_{x \in \mathcal{X}} p_X(x) \int_{z \in \mathcal{Z}} p_Y(Y = z - x) \log(p_Y(Y = z - x)) dx dz \\
&= - \int_{x \in \mathcal{X}} p_X(x) dx \int_{y \in \mathcal{Y}} p_Y(Y = y) \log(p_Y(Y = y)) dy \\
&= h(Y),
\end{aligned}$$

and similar we have $h(Z|Y) = h(X)$. Therefore,

$$h(X + Y) = I(Z, X) + h(Z|X) = I(Z, X) + h(Y) \geq h(Y) \quad (18)$$

$$h(X + Y) = I(Z, Y) + h(Z|Y) = I(Z, Y) + h(X) \geq h(X). \quad (19)$$

This completes the proof. \square

Lemma A.3. *If X and Y are discrete random variables that are independent with the supports satisfying $2 \leq |\mathcal{X}| < \infty, 2 \leq |\mathcal{Y}| < \infty$, then*

$$H(X + Y) > \max\{H(X), H(Y)\}. \quad (20)$$

Proof. From Lemma A.1 and due to the symmetry of X and Y , we only need to prove $H(X + Y) \neq H(X)$. The proof is by contradiction. Suppose $H(X + Y) = H(X)$, then from Eq. 16 follows that $I(X + Y, Y) = 0$, thus $X + Y \perp Y$. However, $\mathbb{P}(Y = y_{\max}|X + Y = x_{\max} + y_{\max}) = 1$, which is different from $\mathbb{P}(Y = y_{\max}) < 1$ (due to $|\mathcal{Y}| \geq 2$). This contradicts $X + Y \perp Y$. \square

Lemma A.4. *If X and Y are continuous random variables that are independent and have a bounded support, then*

$$h(X + Y) > \max\{h(X), h(Y)\}. \quad (21)$$

Proof. From Lemma A.2 and due to the symmetry of X and Y , we only need to prove $h(X + Y) \neq h(X)$. The proof is by contradiction. Suppose $h(X + Y) = h(X)$, then from Eq. 19 follows that $I(X + Y, Y) = 0$, thus $X + Y \perp Y$. For any $\delta > 0$, define an event $\mathcal{M} : x_{\max} + y_{\max} - \delta \leq X + Y \leq x_{\max} + y_{\max}$. If \mathcal{M} occurs, then $Y \geq y_{\max} - \delta$ and $X \geq x_{\max} - \delta$. Thus, $\mathbb{P}_Y(Y \leq y_{\max} - \delta | \mathcal{M}) = 0$. However, we can always choose a $\delta > 0$ that is small enough to make $\mathbb{P}_Y(Y \leq y_{\max} - \delta) > 0$. This contradicts $X + Y \perp Y$. \square

A.2.2 Proof of Theorem 3

Lemma A.5. For any discrete random variable X with its support set as \mathcal{S} , then for any non-injective mapping $f: \mathcal{S} \rightarrow \mathbb{R}$, we have $H(f(X)) < H(X)$, where H is the Shannon entropy.

Proof. We assume the support set \mathcal{S} contains n distinct points $\{x_1, \dots, x_n\}$ with probability $\{p_1, \dots, p_n\}$ respectively, and we assume the support set of $f(X)$ be $\mathcal{S}' = \{x'_1, \dots, x'_m\}$ with m distinct points and the corresponding probability as $\{p'_1, \dots, p'_m\}$. Due to the non-injective property of f , we have $m < n$, and $\{p'_1, \dots, p'_m\}$ is an aggregation clustering of $\{p_1, \dots, p_n\}$. For every positive values of a, b of $c = a + b \leq 1$, we have

$$-c \log c = -(a + b) \log(a + b) = -a \log(a + b) - b \log(a + b) < -a \log a - b \log b \quad (22)$$

Therefore, we have

$$H(f(X)) = \sum_{i=1}^m -p'_i \log p'_i < \sum_{j=1}^n -p_j \log p_j = H(X). \quad (23)$$

□

We first show the proof to the two-dimensional case for intuitive understanding, and then extend the proof to any dimension.

Lemma A.6. For any set of n points $\mathcal{S} = \{\mathbf{x}_1, \dots, \mathbf{x}_n\}$ of each $\mathbf{x}_i \in \mathbb{R}^2$, assume these points are bounded, and are strictly linearly separable by \mathbf{w}^* , i.e., $\text{sgn}(\mathbf{w}^* \cdot \mathbf{x}_i) \neq 0, \forall \mathbf{x}_i \in \mathcal{S}$, and have at least three distinct points (not on the same line). Then, there exists a non-injective linear mapping f from \mathcal{S} to \mathbb{R} such that $\text{sgn}(f(\mathbf{x}_i)) = \text{sgn}(\mathbf{w}^* \cdot \mathbf{x}_i)$ for all $\mathbf{x}_i \in \mathcal{S}$.

Proof. We partition \mathcal{S} to two subsets of $\mathcal{S}_1 = \{\mathbf{x}'_1, \dots, \mathbf{x}'_m\}$ and $\mathcal{S}_2 = \{\mathbf{x}''_1, \dots, \mathbf{x}''_{n-m}\}$ by \mathbf{w}^* . Since $n \geq 3$, without loss of generality, let $m \geq 2$. Due to the \mathcal{S} is bounded set with at least three distinct points not in the same line, we can always find two lines l_1 and l_2 such that any line between l_1 and l_2 separates the two sets of \mathcal{S}_1 and \mathcal{S}_2 and at least one line of l_1 and l_2 (assume l_1) acrosses two distinct points (assume \mathbf{x}'_1 and \mathbf{x}'_2) in the same set of \mathcal{S}_1 or \mathcal{S}_2 (assume \mathcal{S}_1), which is intuitive shown in Fig. A1. Then, we let l be the line that goes through the two points of \mathbf{x}'_1 and \mathbf{x}'_2 , and O' be the intersection point between l_1 and l_2 . Then, we can set up a new coordinate system $O'-x'y'$ with $y' \parallel l$ and $x' \perp y'$. Therefore, there exists a rotation matrix $\mathbf{R} \in \mathbb{R}^{2 \times 2}$ and a translation vector $\mathbf{b} \in \mathbb{R}^2$ such that the coordinate system of $O-xy$ will transform to $O'-x'y'$. Since y' separates the two sets of \mathcal{S}_1 or \mathcal{S}_2 , the first dimension (related to x') of the transformed points would also be separated by y' . Therefore, $f(\mathbf{x}) = \mathbf{R}[1, :] \mathbf{x} + \mathbf{b}[1]$ would be a non-injection linear function, which maps \mathbf{x}'_1 and \mathbf{x}'_2 to the same point, and we also have $\text{sgn}(f(\mathbf{x}_i)) = \text{sgn}(\mathbf{w}^* \cdot \mathbf{x}_i)$ for all $\mathbf{x}_i \in \mathcal{S}$. □

We now begin to prove Theorem 3. We first state that again for convenience.

Theorem A.1. Following Assumption 1, assume that a) the invariant features are strictly separable, bounded, and satisfy support overlap (Assumptions 2, 4, and 5 hold), b) the invariant features are discrete variables with at least three distinct points (not on the same line) and support overlap in each training environment. Then, there exists at least one pair of $(\mathbf{w} \in \mathbb{R}^m, b \in \mathbb{R})$ such that the transformed variables $T_{inv}^e = \mathbf{w} \cdot \mathbf{Z}_{inv}^e + b$ are still bounded and satisfy support overlap, and satisfy $\text{sgn}(T_{inv}^e) = \text{sgn}(\mathbf{w}_{inv}^* \cdot \mathbf{Z}_{inv}^e)$ and $H(T_{inv}^e) < H(\mathbf{Z}_{inv}^e)$ for any $e \in \mathcal{E}_{tr}$.

Proof. For each $z_{inv} \in \cup_{e \in \mathcal{E}_{tr}} \mathbf{Z}_{inv}^e$ define $y^* = \text{sgn}(\mathbf{w}_{inv}^* \cdot z_{inv})$. From the definition of Assumption 5, it follows that $\exists c > 0$ such that $\forall z_{inv} \in \cup_{e \in \mathcal{E}_{tr}} \mathbf{Z}_{inv}^e$

$$y^*(\mathbf{w}_{inv}^* \cdot z_{inv}) \geq c. \quad (24)$$

Next, we choose m vectors of $\{\gamma_1, \dots, \gamma_m\}$ from \mathbb{R}^m such that $\text{Rank}([\mathbf{w}_{inv}^* + \gamma_1; \dots; \mathbf{w}_{inv}^* + \gamma_m]) = m$. Then, for any $i \in [1, m]$, we have

$$y^*((\mathbf{w}_{inv}^* + \gamma_i) \cdot z_{inv}) = y^*(\mathbf{w}_{inv}^* \cdot z_{inv}) + y^*(\gamma_i \cdot z_{inv}) \quad (25)$$

$$\geq y^*(\mathbf{w}_{inv}^* \cdot z_{inv}) - |y^*(\gamma_i \cdot z_{inv})| \quad (26)$$

$$\geq y^*(\mathbf{w}_{inv}^* \cdot z_{inv}) - \|\gamma_i\| \|z_{inv}\| \quad (27)$$

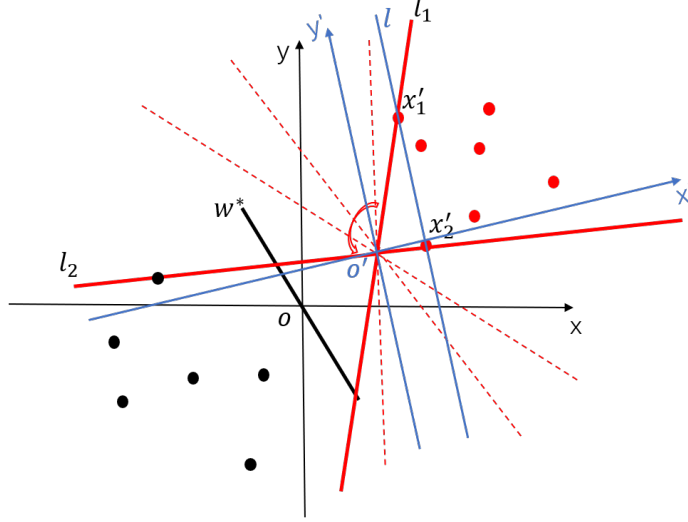


Figure A1: Example proof of Lemma A.6.

Since the support of invariant features is bounded, i.e., there exists a $M > 0$, such that $\|z_{inv}\| < M$. We can always set the magnitude of γ_i to sufficiently small to make $\|\gamma_i\| \leq \frac{c}{2M}$ for each γ_i . Then, we have

$$y^*((w_{inv}^* + \gamma_i) \cdot z_{inv}) \geq \frac{c}{2} > 0, \forall i \in [1, m] \quad (28)$$

Therefore, we can always find m hyperplanes of $\{w_1^*, \dots, w_m^*\}$ such that $\text{sgn}(w_{inv}^* \cdot z_{inv}) = \text{sgn}(w_i^* \cdot z_{inv})$ for any $i \in [1, m]$ and $\text{Rank}([w_1^*; \dots; w_m^*]) = m$. From the assumption, there are three distinct points denoted as z_1, z_2, z_3 that are not in the same line. Next, we would show that there exist at least two $w_k^*, w_j^* \in \{w_1^*, \dots, w_m^*\}$ such that $z'_1 = W'z_1, z'_2 = W'z_2, z'_3 = W'z_3$ with $W' = [w_k^*; w_j^*]$ are still not in the same line. The proof is by contradiction. Assume $z'_1, z'_2, z'_3 \in \mathbb{R}^2$ are in the same line for any two $w_k^*, w_j^* \in \{w_1^*, \dots, w_m^*\}$, then there exists a $r \in \mathbb{R}$ such that $Wz_1 - Wz_2 = r(Wz_1 - Wz_3)$, i.e., $W(z_1 - z_2 - r(z_1 - z_3)) = \mathbf{0}$, where $W = [w_1^*; \dots; w_m^*]$. However, due to $z_1 - z_2 - r(z_1 - z_3) \neq \mathbf{0}$ and $\text{Rank}(W) = m$, this is impossible.

Now, for each environment e , we first transform the variable Z_{inv}^e to $Z' = W'Z_{inv}^e$. Therefore the support set of Z' has at least three points not in the same line, and clearly, $\text{sgn}(w' \cdot Z') = \text{sgn}(w^* \cdot Z_{inv}^e)$ for any $w' \in \mathbb{R}_{++}^2$. Since the support set of invariant features are the same in different environments, the support set of Z' would also be the same in all environments. Now applying the Lemma A.6 to the support set of Z' , there exists a non-injective linear function $f(z) = w''z + b''$ such that $\text{sgn}(f(Z')) = \text{sgn}(w' \cdot Z')$. Let $w = w''W'$ and $b = b''$, then there exists a non-injective linear mapping $T_{inv}^e = w \cdot Z_{inv}^e + b$ from $\cup_{e \in \mathcal{E}_{tr}} Z_{inv}^e$ to \mathbb{R} such that $\text{sgn}(T_{inv}^e) = \text{sgn}(w_{inv}^* \cdot Z_{inv}^e)$ for any $e \in \mathcal{E}_{tr}$. Then from Lemma A.5, we have $H(T_{inv}^e) < H(Z_{inv}^e)$ for any $e \in \mathcal{E}_{tr}$. Since Z_{inv}^e is bounded and satisfies support overlap, T_{inv}^e would be still bounded and satisfies support overlap due to the linear mapping. \square

A.2.3 Proof of Theorem 4

We state the Theorem 4 here for convenience.

Theorem A.2. *Following Assumption 1 or 7, if two sets $\cup_{e \in \mathcal{E}_{tr}} Z_{spu}^e(Y^e = 1)$ and $\cup_{e \in \mathcal{E}_{tr}} Z_{spu}^e(Y^e = -1/0)$ are linearly separable and $H(Z_{inv}^e) > H(Z_{spu}^e)$ on each training environment e , then IB-IRM (and IRM, ERM, or IB-ERM) with any $r^{th} \in \mathbb{R}$ fails to address the OOD generalization problem (Eq. (1)).*

Proof. The proof is trivial. Since two sets $\cup_{e \in \mathcal{E}_{tr}} Z_{spu}^e(Y^e = 1)$ and $\cup_{e \in \mathcal{E}_{tr}} Z_{spu}^e(Y^e = -1/0)$ are linearly separable, there exists a lineal classifier w that only relies on spurious features and can achieve zero classification error on each environment. Therefore, w is an invariant predictor across different training environments. Also, $H(Z_{inv}^e) > H(Z_{spu}^e)$ would make IB-IRM prefer to choose these spurious features. Therefore, w would be an optimal solution of IB-IRM, ERM, IRM, and IB-ERM. However, since w

relies on spurious features which may change arbitrary in unseen environments, it thus fails to solve OOD generalization. \square

A.2.4 Proof of Theorem 5

We state the **CSIB** algorithm here for convenience (set Φ' be the identical matrix initially).

Step 1 (IB-ERM): Apply IB-ERM algorithm to all the training environment data \mathcal{E}_{tr} as:

$$\min_{w, \Phi} \sum_{e \in \mathcal{E}_{tr}} h^e(\Phi) \quad \text{s.t.} \quad \frac{1}{|\mathcal{E}_{tr}|} \sum_{e \in \mathcal{E}_{tr}} R^e(w \cdot \Phi) \leq r^{th} \quad (29)$$

with l the 0-1 loss function.

Step 2 (SVD decomposition): Assume $\Phi^* \in \mathbb{R}^{c \times d}$ and w^* are the feature extractor and classifier learned by IB-ERM and the rank of Φ^* is r . We first do singular value decomposition (SVD) to Φ^* and get $\Phi^* = U\Lambda V^T$ with orthogonal matrixes $U \in \mathbb{R}^{c \times c}$ and $V \in \mathbb{R}^{d \times d}$, which can be partitioned by $\Phi^* = [U_1, U_2][\Lambda_1, \mathbf{0}; \mathbf{0}, \mathbf{0}][V_1^T; V_2^T]$ with $U_1 \in \mathbb{R}^{c \times r}$ and $U_2 \in \mathbb{R}^{c \times (d-r)}$, $\Lambda_1 \in \mathbb{R}^{r \times r}$ is the diagonal matrix with r non-zero elements, and $V_1^T \in \mathbb{R}^{r \times d}$ and $V_2^T \in \mathbb{R}^{(d-r) \times d}$.

Step 3 (Intervention): Pick a random sample $x \in \mathbb{R}^d$ from training environment with ground truth label y . Assume input data is bounded by M , then construct two new features z^1 and z^2 by do operation: $do(z_{1:r}^1) = [-M, \dots, -M]$ and $do(z_{r+1:d}^1) = V_2^T x$; $do(z_{1:r}^2) = [M, \dots, M]$ and $do(z_{r+1:d}^2) = V_2^T x$. Backward the new features z^1 and z^2 to the input space as $x^1 = Vz^1$ and $x^2 = Vz^2$. If the label of x^1 is different from that of x^2 , then end the algorithm and return feature extractor $\Phi^* = \Phi^* \Phi'$ and classifier w^* , otherwise set $\Phi' = V_2^T \Phi'$, and update the environment data variable $X^e = V_2^T X^e$ for each e and then go to the **Step 1**.

Theorem A.3 (Guarantee of CSIB). *Suppose each $e \in \mathcal{E}_{all}$ follows Assumption 1 or 7 with S the orthogonal (invertible) transformation. Assume that the invariant features are strictly separable (5), bounded (Assumptions 2), and satisfy Assumptions 6. Also, for each $e \in \mathcal{E}_{tr}$ in Assumption 1, $Z_{spu}^e \leftarrow AZ_{inv}^e + W^e$ with $A \in \mathbb{R}^{o \times m}$ and $W^e \in \mathbb{R}^o$ or $Z_{inv}^e \leftarrow AZ_{spu}^e + W^e$ with $A \in \mathbb{R}^{m \times o}$ and $W^e \in \mathbb{R}^m$, where W^e is continuous (or discrete variable with each component at least two distinct values), bounded, and zero mean. Each solution to CSIB with l as 0-1 loss, $c \geq m$, and $r^{th} = q$ solves the OOD generalization (Eq. 1).*

Proof. Assume $\Phi^* \in \mathbb{R}^{c \times d}$ and w^* are the feature extractor and classifier learned by IB-ERM. Consider the feature variable extracted by Φ^* as

$$\Phi^* X^e = \Phi^* S(Z_{inv}^e, Z_{spu}^e) = \Phi_{inv} Z_{inv}^e + \Phi_{spu} Z_{spu}^e. \quad (30)$$

We first show that $\Phi_{inv} = \mathbf{0}$ or $\Phi_{spu} = \mathbf{0}$. We prove this by contradiction. Assume $\Phi_{inv} \neq \mathbf{0}$ and $\Phi_{spu} \neq \mathbf{0}$. By observing that a solution of $\Phi_{inv} = \mathbf{1}, \Phi_{spu} = \mathbf{0}, w^* = w_{inv}^*$ could make the average training error to q , therefore any solution returned by IB-ERM should also achieve the error no larger than q (because $r^{th} = q$ in the constraint of Eq. 29). Therefore $w^* \neq \mathbf{0}$.

1. In the case when each $e \in \mathcal{E}_{tr}$ follows Assumption 1 of $Z_{spu}^e \leftarrow AZ_{inv}^e + W^e$, we have

$$\begin{aligned} w^* \cdot (\Phi_{inv} Z_{inv}^e + \Phi_{spu} Z_{spu}^e) &= w^* \cdot \Phi_{inv} Z_{inv}^e + w^* \cdot \Phi_{spu} (AZ_{inv}^e + W^e) \\ &= w^* \cdot (\Phi_{inv} + \Phi_{spu} A) Z_{inv}^e + w^* \cdot \Phi_{spu} W^e. \end{aligned}$$

Then, for any $z = (z_{inv}^e, z_{spu}^e)$ of $\mathbf{1}(w_{inv}^* \cdot z_{inv}^e) = 1$, we must have $w^* \cdot (\Phi_{inv} + \Phi_{spu} A) z_{inv}^e + w^* \cdot \Phi_{spu} W^e \geq 0$ for any W^e to make error no larger than q . Since W^e is zero mean with at least two distinct points, we can conclude that $w^* \cdot (\Phi_{inv} + \Phi_{spu} A) z_{inv}^e \geq 0$; Similarly, for any $z = (z_{inv}^e, z_{spu}^e)$ of $\mathbf{1}(w_{inv}^* \cdot z_{inv}^e) = 0$, we have $w^* \cdot (\Phi_{inv} + \Phi_{spu} A) z_{inv}^e < 0$. From Lemma A.3 or Lemma A.4, we get $H((\Phi_{inv} + \Phi_{spu} A) Z_{inv}^e + \Phi_{spu} W^e) > H((\Phi_{inv} + \Phi_{spu} A) Z_{inv}^e)$. Therefore, there exists a more optimal solution to IB-ERM with zero weight to Z_{spu}^e , which contradicts the assumption.

2. In the case when each $e \in \mathcal{E}_{tr}$ follows Assumption 1 of $Z_{inv}^e \leftarrow AZ_{spu}^e + W^e$, we have

$$\begin{aligned} w^* \cdot (\Phi_{inv} Z_{inv}^e + \Phi_{spu} Z_{spu}^e) &= w^* \cdot \Phi_{inv} (AZ_{spu}^e + W^e) + w^* \cdot \Phi_{spu} Z_{spu}^e \\ &= w^* \cdot (\Phi_{spu} + \Phi_{inv} A) Z_{spu}^e + w^* \cdot \Phi_{inv} W^e. \end{aligned}$$

Then, for any $z = (z_{inv}^e, z_{spu}^e)$ of $\mathbf{1}(w_{inv}^* \cdot z_{inv}^e) = 1$, we must have $w^* \cdot (\Phi_{spu} + \Phi_{inv}A)z_{spu}^e + w^* \cdot \Phi_{inv}w^e \geq 0$ for any w^e to make error no larger than q . Since W^e is zero mean with at least two distinct points, we can conclude that $w^* \cdot (\Phi_{spu} + \Phi_{inv}A)z_{spu}^e \geq 0$; Similarly, for any $z = (z_{inv}^e, z_{spu}^e)$ of $\mathbf{1}(w_{inv}^* \cdot z_{inv}^e) = 0$, we have $w^* \cdot (\Phi_{spu} + \Phi_{inv}A)z_{spu}^e < 0$. From Lemma A.3 or Lemma A.4, we get $H((\Phi_{spu} + \Phi_{inv}A)Z_{spu}^e + \Phi_{inv}W^e) > H((\Phi_{spu} + \Phi_{inv}A)Z_{spu}^e)$. Therefore, there exists a more optimal solution to IB-ERM with zero weight to Z_{inv}^e , which contradicts the assumption.

3. In the case when each $e \in \mathcal{E}_{tr}$ follows Assumption 7 of $Z_{spu}^e = AY^e + W^e$, we have

$$\begin{aligned} w^* \cdot (\Phi_{inv}Z_{inv}^e + \Phi_{spu}Z_{spu}^e) &= w^* \cdot \Phi_{inv}Z_{inv}^e + w^* \cdot \Phi_{spu}(AY^e + W^e) \\ &= w^* \cdot \Phi_{inv}Z_{inv}^e + w^* \cdot \Phi_{spu}AY^e + w^* \cdot \Phi_{spu}W^e. \end{aligned}$$

Then, if $\mathbb{P}(w^* \cdot \Phi_{spu}AY^e + w^* \cdot \Phi_{spu}W^e \geq 0|Y^e = 1)\mathbb{P}(Y^e = 1) + \mathbb{P}(w^* \cdot \Phi_{spu}AY^e + w^* \cdot \Phi_{spu}W^e < 0|Y^e = -1)\mathbb{P}(Y^e = -1) \geq 1 - q$, then there exists a more optimal solution to IB-ERM with zero weight to Z_{inv}^e . This is because, $H(\Phi_{inv}Z_{inv}^e + \Phi_{spu}AY^e + \Phi_{spu}W^e|Y^e = 1) > H(\Phi_{spu}AY^e + \Phi_{spu}W^e|Y^e = 1)$ and $H(\Phi_{inv}Z_{inv}^e + \Phi_{spu}AY^e + \Phi_{spu}W^e|Y^e = -1) > H(\Phi_{spu}AY^e + \Phi_{spu}W^e|Y^e = -1)$ from Lemma A.3 or Lemma A.4. Thus, this contradicts the assumption.

Otherwise if $\mathbb{P}(w^* \cdot \Phi_{spu}AY^e + w^* \cdot \Phi_{spu}W^e \geq 0|Y^e = 1)\mathbb{P}(Y^e = 1) + \mathbb{P}(w^* \cdot \Phi_{spu}AY^e + w^* \cdot \Phi_{spu}W^e < 0|Y^e = -1)\mathbb{P}(Y^e = -1) < 1 - q$, then, for any $z = (z_{inv}^e, z_{spu}^e)$ of $\mathbf{1}(w_{inv}^* \cdot z_{inv}^e) = 1$, we must have $w^* \cdot \Phi_{inv}z_{inv}^e + w^* \cdot \Phi_{spu}Ay^e + w^* \cdot \Phi_{spu}w^e \geq 0$ for any y^e and w^e to make error no larger than q . Since $\mathbb{P}(w^* \cdot \Phi_{spu}AY^e + w^* \cdot \Phi_{spu}W^e < 0|z_{inv}^e) > 0$, we can conclude that $w^* \cdot \Phi_{inv}z_{inv}^e \geq 0$. Similarly, for any $z = (z_{inv}^e, z_{spu}^e)$ of $\mathbf{1}(w_{inv}^* \cdot z_{inv}^e) = 0$, we have $w^* \cdot \Phi_{inv}z_{inv}^e < 0$. Also, due to the positive correlation between $w^* \cdot \Phi_{inv}Z_{inv}^e$ and $w^* \cdot \Phi_{spu}AY^e$ in this case, we have $H(\Phi_{inv}Z_{inv}^e) \leq H(\Phi_{inv}Z_{inv}^e + \Phi_{spu}AY^e)$. Follows Lemma A.3 or Lemma A.4, we get $H(\Phi_{inv}Z_{inv}^e + \Phi_{spu}AY^e) < H(\Phi_{inv}Z_{inv}^e + \Phi_{spu}AY^e + \Phi_{spu}W^e)$, which follows that $H(\Phi_{inv}Z_{inv}^e) < H(\Phi_{inv}Z_{inv}^e + \Phi_{spu}AY^e + \Phi_{spu}W^e)$. Therefore, there exists a more optimal solution to IB-ERM with zero weight to Z_{spu}^e , which contradicts the assumption.

From now, we have proved that the feature extractor Φ^* learned by IB-ERM would never extract both spurious features and invariant features together. Then, we perform singular value decomposition (SVD) to the Φ^* as

$$\Phi^* = U\Lambda V^T = [U_1, U_2][\Lambda_1, \mathbf{0}; \mathbf{0}, \mathbf{0}][V_1^T; V_2^T] = U_1\Lambda_1V_1^T \quad (31)$$

Let $S \in \mathbb{R}^{d \times d}$ be the orthogonal matrix. Set r be the rank of the matrix Φ^* , i.e., $r = \text{Rank}(\Phi^*)$, and let $V_1^T S = [V'_1, V'_2]$ with $V'_1 \in \mathbb{R}^{r \times m}$ and $V'_2 \in \mathbb{R}^{r \times o}$, and $V_2^T S = [V''_1, V''_2]$ with $V''_1 \in \mathbb{R}^{(d-r) \times m}$ and $V''_2 \in \mathbb{R}^{(d-r) \times o}$, then

$$\Phi^* X^e = U_1\Lambda_1V_1^T S[Z_{inv}^e; Z_{spu}^e] = U_1\Lambda_1(V'_1Z_{inv}^e + V'_2Z_{spu}^e). \quad (32)$$

Since $\Phi^* X^e$ contains the information either from spurious features or from invariant features, we must have $U_1\Lambda_1V'_1 = \mathbf{0}$ or $U_1\Lambda_1V'_2 = \mathbf{0}$, and thus, $V'_1 = \mathbf{0}$ or $V'_2 = \mathbf{0}$ due to $\text{Rank}(U_1\Lambda_1) = r$. If $V'_2 = \mathbf{0}$, then Φ^* extract invariant features only. Otherwise when $V'_1 = \mathbf{0}$, we decompose the $V^T S$ by

$$V^T S = [V_1^T; V_2^T]S = [V_1^T S; V_2^T S] = [V'_1, V'_2; V''_1, V''_2]. \quad (33)$$

Since V^T and S are both the orthogonal matrix, $V^T S$ is also orthogonal, thus $V'_1 = \mathbf{0} \Rightarrow V_2^T V''_2 = \mathbf{0}$, and then $\text{Rank}(V''_2) = \text{Rank}([V'_2; V''_2]) - \text{Rank}(V'_2) = o - r$ (note that $r \leq \min\{m, o\}$). Then,

$$V_2^T X^e = V_2^T S[Z_{inv}^e; Z_{spu}^e] = [V''_1, V''_2][Z_{inv}^e; Z_{spu}^e] = V''_1Z_{inv}^e + V''_2Z_{spu}^e. \quad (34)$$

Therefore, by running the CSIB for one iteration, the rank of spurious features would be decreased by $r > 0$. This would result in zero weight to spurious features by finite runs of CSIB.

Then, we tend to show why the intervention step could help to distinguish whether V'_1 is $\mathbf{0}$ or not. For a specific instance $x = S[z_{inv}; z_{spu}]$, let two new features be z^1 and z^2 , then $do(z_{1:r}^1) = [-M, \dots, -M]$ and $do(z_{r+1:d}^1) = V_2^T x$; $do(z_{1:r}^2) = [M, \dots, M]$ and $do(z_{r+1:d}^2) = V_2^T x$. Back the new features z^1 and z^2

to the input space as $x^1 = Vz^1$ and $x^2 = Vz^2$. If $V'_1 = \mathbf{0}$, then

$$\begin{aligned} S^{-1}x^1 &= S^{-1}Vz^1 = S^{-1}V[z_{1:r}^1; V_1''z_{inv} + V_2''z_{spu}] \\ &= (V^TS)^T[z_{1:r}^1; V_1''z_{inv} + V_2''z_{spu}] \\ &= [V_1'^T, V_1''^T; V_2'^T, V_2''^T][z_{1:r}^1; V_1''z_{inv} + V_2''z_{spu}] \\ &= [V_1'^T z_{1:r}^1 + V_1''^T(V_1''z_{inv} + V_2''z_{spu}); V_2'^T z_{1:r}^1 + V_2''^T(V_1''z_{inv} + V_2''z_{spu})] \\ &= [z_{inv}; V_2'^T z_{1:r}^1 + V_2''^T V_2''z_{spu}], \end{aligned}$$

and similar we have $S^{-1}x^2 = [z_{inv}; V_2'^T z_{1:r}^2 + V_2''^T V_2''z_{spu}]$. Therefore, the ground truths of x^1 and x^2 are the same. On other hand, if $V'_1 \neq \mathbf{0}$, then $V'_2 = \mathbf{0}$, and

$$\begin{aligned} S^{-1}x^1 &= S^{-1}Vz^1 = S^{-1}V[z_{1:r}^1; V_1''z_{inv} + V_2''z_{spu}] \\ &= (V^TS)^T[z_{1:r}^1; V_1''z_{inv} + V_2''z_{spu}] \\ &= [V_1'^T, V_1''^T; V_2'^T, V_2''^T][z_{1:r}^1; V_1''z_{inv} + V_2''z_{spu}] \\ &= [V_1'^T z_{1:r}^1 + V_1''^T(V_1''z_{inv} + V_2''z_{spu}); V_2'^T z_{1:r}^1 + V_2''^T(V_1''z_{inv} + V_2''z_{spu})] \\ &= [V_1'^T z_{1:r}^1 + V_1''^T V_1''z_{inv}; z_{spu}], \end{aligned}$$

and similar we have $S^{-1}x^2 = [V_1'^T z_{1:r}^2 + V_1''^T V_1''z_{inv}; z_{spu}]$. Since $z_{1:r}^1 = -z_{1:r}^2$ and their magnitudes are larger enough to make $\text{sgn}(w_{inv}^* \cdot (V_1'^T z_{1:r}^1 + V_1''^T V_1''z_{inv})) \neq \text{sgn}(w_{inv}^* \cdot (V_1'^T z_{1:r}^2 + V_1''^T V_1''z_{inv}))$, the ground truths of x^1 and x^2 would be different. Therefore, the intervention step could help to detect whether invariant features or spurious features are extracted by using a single sample only.

Finally, when only invariant features are learned by CSIB, the training error is minimized, i.e., $w^*\Phi_{inv} \in \arg\min_f \mathbb{E}_{\mathbb{P}^{tr}}[l((X_{inv}, Y), f)]$. Then, based on our assumption to the invariant features (Assumptions 6), i.e., $\forall e \in \mathcal{E}_{all}, A_l(\mathbb{P}_{inv}^{tr}) \subseteq A_l(\mathbb{P}_{inv}^e)$, therefore, for any $e \in \mathcal{E}_{all}$, we have $\mathbb{E}_{\mathbb{P}^e}[l((X, Y), w^*\Phi)] = \mathbb{E}_{\mathbb{P}^e}[l((X_{inv}, Y), w^*\Phi_{inv})] = \mathbb{E}_{\mathbb{P}^{tr}}[l((X_{inv}, Y), w^*\Phi_{inv})] = q$. \square

It is worth to note that as we can see, the proof of Theorem A.3 do not relies on how many labels there would be, so it also holds when applying to multi-class classification task as long as the corresponding assumptions and conditions are satisfied.

A.2.5 Proof of the invariant predictor in Example 3

Here, we would show that why the resulting predictor of case 1) of $\Phi_{inv} = 0$ and $\Phi_{spu} = 1$ in Example 3 is an invariant predictor across training environments. This is because, for the first environment of $W^e = -0.4/0.4$, we have

$$\begin{aligned} \mathbb{E}[Y^e | Z_{spu}^e = a] &= \mathbb{P}(Y^e = 1 | Z_{spu}^e = a) - \mathbb{P}(Y^e = -1 | Z_{spu}^e = a) \\ &= \frac{\mathbb{P}(Y^e = 1, Z_{spu}^e = a) - \mathbb{P}(Y^e = -1, Z_{spu}^e = a)}{\mathbb{P}(Y^e = 1, Z_{spu}^e = a) + \mathbb{P}(Y^e = -1, Z_{spu}^e = a)} \\ &= \frac{\mathbb{P}(Z_{spu}^e = a | Y^e = 1)\mathbb{P}(Y^e = 1) - \mathbb{P}(Z_{spu}^e = a | Y^e = -1)\mathbb{P}(Y^e = -1)}{\mathbb{P}(Z_{spu}^e = a | Y^e = 1)\mathbb{P}(Y^e = 1) + \mathbb{P}(Z_{spu}^e = a | Y^e = -1)\mathbb{P}(Y^e = -1)} \\ &= \begin{cases} 1, & a = 0.6 \text{ or } 1.4 \\ -1, & a = -1.4 \text{ or } -0.6 \\ \text{undefined}, & a \neq -1.4 \text{ and } a \neq -0.6 \text{ and } a \neq 0.6 \text{ and } a \neq 1.4 \end{cases} \end{aligned}$$

For the second environment of $W^e = -0.3/0.3$, we have

$$\begin{aligned} \mathbb{E}[Y^e | Z_{spu}^e = a] &= \mathbb{P}(Y^e = 1 | Z_{spu}^e = a) - \mathbb{P}(Y^e = -1 | Z_{spu}^e = a) \\ &= \frac{\mathbb{P}(Y^e = 1, Z_{spu}^e = a) - \mathbb{P}(Y^e = -1, Z_{spu}^e = a)}{\mathbb{P}(Y^e = 1, Z_{spu}^e = a) + \mathbb{P}(Y^e = -1, Z_{spu}^e = a)} \\ &= \frac{\mathbb{P}(Z_{spu}^e = a | Y^e = 1)\mathbb{P}(Y^e = 1) - \mathbb{P}(Z_{spu}^e = a | Y^e = -1)\mathbb{P}(Y^e = -1)}{\mathbb{P}(Z_{spu}^e = a | Y^e = 1)\mathbb{P}(Y^e = 1) + \mathbb{P}(Z_{spu}^e = a | Y^e = -1)\mathbb{P}(Y^e = -1)} \\ &= \begin{cases} 1, & a = 0.7 \text{ or } 1.3 \\ -1, & a = -1.3 \text{ or } -0.7 \\ \text{undefined}, & a \neq -1.3 \text{ and } a \neq -0.7 \text{ and } a \neq 0.7 \text{ and } a \neq 1.3 \end{cases} \end{aligned}$$

Therefore, the predictor of $\Phi_{inv} = 0$ and $\Phi_{spu} = 1$ would make $\mathbb{E}[Y^e | Z_{spu}^e = a]$ invariant across two training environments for any $a \in \mathbb{R}$, and thus is an invariant predictor. Actually, any predictor of zero training error is an invariant predictor across training environments.